SPECTRUM ADAPTATION ACROSS LINK AND NETWORK

Approved by:

Dr. Dr. Joseph Camp

Dr. Dinesh Rajan

Dr. Eli Olinick

Dr. TBA1

Dr. TBA2

SPECTRUM ADAPTATION ACROSS LINK AND NETWORK

A Dissertation Presented to the Graduate Faculty of the

Bobby B. Lyle School of Engineering

Southern Methodist University

in

Partial Fulfillment of the Requirements

for the degree of

Doctor of Philosophy

with a

Major in Electrical Engineering

by

Pengfei Cui

(B.S., Beijing Institute of Technology, 2007)
(M.S., University of Chinese Academy of Sciences, 2010)

TBA

ACKNOWLEDGMENTS

TBA

Cui , Pengfei B.S., Beijing Institute of Technology, 2007
M.S., University of Chinese Academy of Sciences, 2010

Spectrum Adaptation across Link and Network

Advisor: Professor Dr. Joseph Camp

Doctor of Philosophy degree conferred TBA
Dissertation completed TBA

Due to the convenience of deployment and utility, wireless devices and network has become the dominant tools for telecommunication. However, the spectrum resource is limited in natural and has to be approved for accessibility, there is a huge challenge for individual devices and infrastructure to efficiently exploit the licensed frequency. In 2009, the FCC has approved the use of broadband services in the white space of UHF TV bands, which were formerly exclusively licensed to television broadcasters. These white space bands are now available for unlicensed public use, offerring new opportunities for new design of device and network with better performance in throughput and economy cost. In this work, we investigate multiband adaptation in both link communication and network deployment. Furthermore, we design algorithms with in-field measurement to improve the link and network performance. First, we leverage knowledge of in-situ operation across frequency bands with real-time measurements of the activity level to select the the band with the highest throughput. To do so, we perform a number of experiments in typical vehicular topologies. With two models based on machine learning algorithms and an in-situ training set, we predict the throughput based on: (*i.*) prior performance for similar context information (*e.g.*, SNR, GPS, relative speed, and link distance), and (*ii.*) real-time activity level and relative channel quality per band. In the field, we show that training on a repeatable route with these machine learning techniques can yield vast performance improvements from prior schemes. Second, we measure the spectrum utility in the Dallas-Fort Worth metropolitan and surrounding areas and propose a

measurement-driven band selection framework, Multiband Access Point Estimation (MAPE). In particular, we study the white space and WiFi bands with in-field spectrum utility measurements, revealing the number of access points required for an area with channels in multiple bands. In doing so, we find that networks with white space bands reduce the number of access points by up to 1650% in sparse rural areas over similar WiFi-only solutions. In more populated rural areas and sparse urban areas, we find an access point reduction of 660% and 412%, respectively. However, due to the heavy use of white space bands in dense urban areas, the cost reductions invert (an increase in required access points of 6%). Finally, we numerically analyze band combinations in typical rural and urban areas and show the critical factor that leads to cost reduction: considering the same total number of channels, as more channels are available in the white space bands, less access points are required for a given area. Furthermore, we model the heterogeneous white space and WiFi access tier deployment problem. We propose a relaxed ILP to get the lower bound of the amount of access point under resource limitations and a heuristic approach of the problem. We start from the uniform population distribution wireless network deployment, then discuss the non-uniform population distribution wireless network deployment. Then, we discuss white space band application in multiple spectrum resource degree. In particular, we map the problem as a Bin packing problem and resolve it with Multiband Hetegeneous Access Point deployment method. In doing so, we discuss the benefit of white space bands in reducing the number of acess points and provide heuristic solution for access point selection. Our numerical simulation shows that hetergeneous access point could benefit most of the scenarios in wireless access tier deployment. Forth, we present an integer linear programming model to leverage diverse prop- agation characteristics of white space and WiFi bands to deploy optimal WhiteMesh networks. Since such optimization is known to be NP-hard,

we design a heuristic algorithm, Band-based Path Selection (BPS), which we show approaches the performance of the optimal solution with reduced complexity. We additionally compare the performance of BPS against two well-known multi- channel, multi-radio deployment algorithms across a range of scenarios spanning those typical for rural areas to urban areas. In doing so, we achieve between 3 to 6 times the gateway goodput of these existing multi-channel, multi-radio algorithms, which are agnostic to diverse propagation characteristics across bands. Moreover, we show that, with similar channel resources and bandwidth, the joint use of WiFi and white space bands can achieve a served user demand of 170% that of mesh networks with only WiFi bands or white space bands, respectively. Lastly, we propose to discuss the beamforming application in large scale network deployment. Beamforming is a efficient way to increase the spatial reuse. With the application of beaforming, a single access point could communicate with multiple device simultaneously. In large scale network deployment, beamforming could increase the capacity of an access point and lower the cost through reducing the number of access points. In our work, we will investigate in what degree the beamforming could benifet the vendors in wireless network deployment.

TABLE OF CONTENTS

LIST OF FIGURES

LIST OF TABLES

Write something here. I dedicate this thesis to someone important to me.

Chapter 1

Introduction

Wireless network is the most convenient method to get service for users. The demand of wireless device users inspires vendors to provide faster, stable service in their networks. Because of the prevalence of individual devices, vehicular wireless devices and wireless sensors, wireless data traffic is expected to increasde a thousand-fold over the next decade [1], greatly motivating the improvement of link communication and network deployment.

However, unlike wired networks, wireless devices have to share crowd and unstable channels in limited frequencies. Especially in vehicular environment, the situation is even worse due to the moving. Fortunately, drivers and passengers around the world could utilize a wide array of vehicular applications ranging from real-time traffic monitoring and safety applications to various infotainment applications. However, the continuous use of such applications is limited due to the challenge of transmitting over highly-dynamic vehicular wireless channels. In such networks, the increasing availability of different frequency bands with correspondingly diverse propagation characteristics could allow flexibility and robustness of vehicular links. Even with spectral flexibility, links are extremely tenuous, demanding instantaneous decisions to remain connected, motivating an algorithm that can find the appropriate frequency band quickly and according to the current environmental context.

Obviously, more frequencies could improve the performance for both link and network communication. The FCC has approved the use of broadband services in the white spaces of UHF TV bands, which were formerly exclusively licensed to television

broadcasters. These white space bands are now available for unlicensed public use, enabling the deployment of wireless access networks across a broad range of scenarios from sparse rural areas (one of the key applications identified by the FCC) to dense urban areas [31]. The white space bands operate in available channels from 54-806 MHz, having a far greater propagation range than WiFi bands for similar transmission power [16]. In WiFi and white space heterogeneous wireless network, the service area degree of an access point depends on the capacity of radios, the propagation range and the demands of the serving area. The scant frequencies of radios, the propagation distinctive and the demands diversity of population distribution bring the variation of an access point service area. These issues are substantial to designing an optimal network deployment and provide potential commercial wireless services to clients in any location. Thus, the new opportunities created by white spaces motivate the following questions for wireless Internet carriers, which have yet to be addressed: (i) To what degree can white space bands reduce the network deployment cost of sparsely populated rural areas as opposed to comparable WiFi-only solutions? and (ii) Where along the continuum of user population densities do the white space bands no longer offer cost savings for wireless network deployments? and To what degree can hetergeneous access points benefit the dense population areas and sparsely populated rural areas?

White space is not only benefit the access tier network, but also benefit the backhual tier networks. About a decade ago, numerous cities solicited proposals from network carriers for exclusive rights to deploy city-wide WiFi, spanning hundreds of square miles. While the vast majority of the resulting awarded contracts used a wireless mesh topology, initial field tests revealed that the actual WiFi propagation could not achieve the proposed mesh node spacing. As a result, many network carriers opted to pay millions of dollars in penalties rather than face the exponentially-increasing

deployment costs (e.g., Houston [50] and Philadelphia [20]). Thus, while a few mesh networks have been deployed in certain communities [19, 10], wireless mesh networks have largely been unsuccessful in achieving the scale of what was once anticipated [35]. Around the same time, the digital TV transition created more spectrum for use with data networks [5]. These white space bands operate in available channels from 54-806 MHz, having increased propagation characteristics as compared to WiFi [16]. Hence, the FCC has identified rural areas as a key application for white space networks since the reduced population from major metropolitan areas allows a greater service area per backhaul device without saturating wireless capacity. Naturally, the question arises for these rural communities as well as more dense urban settings: how can the emerging white space bands improve large-scale mesh network deployments? While much work has been done on deploying multihop wireless networks with multiple channels and radios, the differences in propagation have not be exploited in their models [46, 59, 57], which could be the fundamental issue for the success of mesh networks going forward.

Beamforming is recognized as an prospective technology to further improve the performance of wireless networks, through increasing both time reuse and spatial reuse. However, people still have the question: in what degree beamforming could add capacity and reduce the cost for the network. This is the fundamental issue which could inspire new technology utilization in the wireless networks.

1.1. Challenges

For wireless networks, both the clients and the vendors require better service and low cost. However, due to the nature and policy, wireless channels suffer a lot in providing efficient and stable service for either link communication or network deployments. Spectrum adaptation offers new solution for these issues. However, the

diversity of spectrum and network complexity present great challenges in designing multiband communication systems, for both link and network layers.

First, accurate knowledge of channel status is hard to be detected at the receiver. In recently, cognitive radio mechanisms which interleave channel accesses motivate the frequency band selection problem of finding the optimal spectrum on which to transmit [24]. Prior work has considered a number of challenges in leveraging white space frequencies including spectrum sensing, frequency-agile operation, geolocation, solving stringent spectral mask requirements, and providing reliable service in unlicensed and dynamically changing spectrum [56]. In particular, there has recently been an acceleration in spectrum sensing work [48, 36, 18]. Based on these works, protocols have been built for multi-channel and/or multiband wireless operation [34, 49, 54]. Other works have presented methods for searching for the most efficient transmission channel [40], discovering channel information [48, 54], and estimating channel quality [34]. Moreover, the emergence of a number of diverse sensors on a vehicle motivates work on heterogeneous wireless networks, which have different frequency bands and technologies [30]. Thus, the various communication standards have diverse throughput capacity, allowing the choice of technology to possibly usurp frequency band decisions. For example, an 802.11n link at 5.8 GHz with high levels of loss might still be a better choice than a Bluetooth link at 2.4 GHz with little loss due to the discrepancy of hundreds of Mbps in throughput capacity. While these works have considered spectral activity and developing protocols and algorithms to find spectral holes, less of a focus has been on coupling such information with historical performance in a given propagation environment.

Second, in access layer network deployment, specific to rural areas, the lack of user density and corresponding traffic demand per unit area as compared to dense urban areas allows greater levels of spatial aggregation to reduce the total number

of required access points, lowering network deployment costs. In densely populated urban areas, the greater concentration of users and higher levels of traffic demand can be served by maximizing the spatial reuse. While many works have worked to address multihop wireless network deployment in terms of maximizing served user demand and/or minimizing network costs, the unique propagation characteristics and the interference from coexisting activities in white space bands have either not been jointly studied or assumed to have certain characteristics without explicit measurement [57]. Specifically, previous work has investigated wireless network deployment in terms of gateway placement, channel assignment, and routing [29, 37]. However, each of these works focus on the deployment in WiFi bands without considering the white space bands. Moreover, the assumption of idle channels held in these models fails to match the in-field spectrum utility, which could degrade the performance of a wireless network. These two issues are critical for designing an optimal network deployment and providing commercial wireless services to clients in any location.

Third, in backhual layer, researchers have done both centralized and distributed work for channel assignment and routing [46, 61]. However, FCC's new policy import new diversity to this issue, propagatation difference becomes a new parameter for the optimization. Since the origin problem is already a NP-hard problem, the problem developing from the new white space policy make it more complex. Thus, new channel assignment methods for the multiband scenario is a new question people have to answer.

Lastly, beamforming makes the wireless network similar to the wired network in some degree. However, lacking of protocols and assignment methods make it hard to apply the technology in field. The issues of beamforming in application, such as deafth, new hidden problem need to be leveraged and resolved by new protocols and algorithms. This new technology inspire the optimization more challenging and

meaningful.

1.2. Contributions and Futurework

This work propose spectrum adaptation for both the link communication and network optimization to improve the performance of wireless devices in multiple bands accessiable environment.

In this link spectrum adaptation, we develop multiband adaptation protocols which couple the prior knowledge of in-situ performance of various bands with the instantaneous knowledge of spectral activity, SNR, and current location of each band to arrive at a decision on the optimal band to transmit. To do so, we use an off-the-shelf platform that allows direct comparison and simultaneous experimentation across four different wireless frequency bands from 450 MHz to 5.8 GHz with the same physical and media access layers. We first develop a framework for multiband adaptation using both historical information and instantaneous measurements. This framework is broad enough to study adaptation across licensed and unlicensed bands, including white space frequency bands. We propose two different machine-learning-based multiband adaptation algorithms. The first machine learning algorithm, referred to as the Location-based Look-up Algorithm, is based on the idea of k-nearest-neighbor classification. The second machine-learning-based algorithm uses decision trees for classification. For comparison, we also create two baseline adaptation algorithms which attempt to make the optimal band selection based on only: (i.) historical performance data, and (ii.) instantaneous SNR measurements across various bands. We perform extensive outdoor V-2-V experiments to evaluate the proposed algorithms. Our results indicate that the proposed machine learning based algorithms improve throughput by up to 49.3% over these baseline methods.

In the access layer network deployment, we perform a measurement study which considers the propagation characteristics and observed in-field spectrum availability of white space and WiFi channels to find the total number of access points required to serve a given user demand. Across varying population densities in representative rural and metropolitan areas, we compare the cost savings (defined in terms of number of access points reduced) when white space bands are not used. To do so, we first define the metric to quantify the spectrum utility in a given measurement location. With the in-field measured spectrum utility data in metropolitan and surrounding areas of Dallas-Fort Worth (DFW), we calculate the activity level in WiFi and white space bands. Second, we propose a measurement-driven framework to find the number of access points required for areas with differing population densities according to our measurement locations and census data. We then evaluate our measurement-driven framework, showing the band selection across downtown, residential and university settings in urban and rural areas and analyze the impact of white space and WiFi channel combinations on a wireless deployment in these representative scenarios. The main contributions of our work are as follows: We perform in-field measurements of spectrum utilization in various representative scenarios across the DFW metroplex, ranging from sparse rural to dense urban areas and consider the environmental setting (e.g., downtown, residential, or university campus). We develop a measurement-driven Multi-band Access Point Estimation (MAPE) framework to jointly leverage propagation and spectrum availability of white space and WiFi bands for wireless access networks across settings. We analyze our framework under capacity and coverage constraints to show that, with white space bands, the number of access points can be greatly reduced from WiFi-only deployments by up to 1650% in rural areas. We quantify the impact of white space and WiFi channel combinations to understand the tradeoffs involved in choosing the optimal channel setting, given a certain number of

available channels from multiple bands. Furthermore, we discuss to centralized using frequencies or distributed using them in single access point. Through our numerical simulation, we show that in dense area centralized using spectrum gain more than sparse area.

In the backhual layer network deployment, we leverage the diversity in propagation of white space and WiFi bands in the planning and deployment of large-scale wireless mesh networks. To do so, we first form an integer linear program to jointly exploit white space and WiFi bands for optimal WhiteMesh topologies. Second, since similar problem formulations have been shown to be NP-hard [33], we design a heuristic algorithm, Band-based Path Selection (BPS). We then show the algorithm approaches the performance of the optimal solution but with a reduced complexity. To assess the performance of our scheme, we compare the performance of BPS against two well-known multi-channel, multi-radio deployment algorithms across a wide range of scenarios, including those typical for rural areas as well as urban settings. Finally, we quantify the degree to which the joint use of both band types can improve the performance of wireless mesh networks. We develop an optimization framework based on integer linear programming to jointly leverage white space and WiFi bands to serve the greatest user demand in terms of gateway throughput in wireless mesh networks. We build an algorithm, Band-based Path Selection (BPS), which considers the diverse propagation and overall interference level of WiFi and white space bands using a two-stage approach. In the first stage, we prioritize the bands with the greatest propagation to reduce the overall hop count. In the second stage, we compare the interference level of path choices with similar hop count. We perform extensive analysis across offered loads, network sizes, and WiFi/white space band combinations, showing that BPS outperforms existing multi-channel, multi-radio algorithms techniques by 3 and 6 times in terms of the served user demand. Given similar chan-

nel resources (bandwidth and transmission power), we additionally show that while WiFi-only mesh topologies would largely outperform mesh networks with only white space bands, the joint use of the two types of bands (i.e., WhiteMesh networks) can yield up to 170% of the served user demand compared to mesh networks with only one type of band.

In the beamforming application, we are going to design protocols to optimize the network deployment cost under the limitation of QoS. Through the beamforming, we are going to increase the time reuse in the traditional RTS/CTS link communication and the reduce the cost for network deployment.

1.3. Proposal Overview

In Chapter 2, we discuss the background of this work, including the basic knowledge related to this work and the hardware platform and software tools that we use. Chapter 3 provides an analysis and solution of vehicular link spectrum adaptation for multiband scenario. We also proposed an access layer network deployment framework in Chapter 4 and discuss the optimization of a single access point with spectrum limitation. In Chapter 5, we propose an algorithm to assign channels in multiband scenario for optimizing the throughput performance in backhual networks. In Chapter 6, we discuss the potential beamforming technology application in link communication and networks. Finally, we conclude our work in Chapter 7.

Chapter 2

Background

In this chapter, we describe the background of our research, including the basic technology related to this work and the hardware/software tools that we used to implement and evaluate our proposed algorithms in this work.

2.1. White Space Bands

The white space band term is mentioned the frequencies channels previously used by analog TV broadcasts. In United States, full power analog television broadcasts, which operated between the 54 MHz and 806 MHz television frequencies (Channels 2-69), ceased operating on June 12, 2009 per a United States digital switchover mandate. At that time, full power TV stations were required to switch to digital transmission and operate only between 54 MHz and 698 MHz. [5]

Industry and academia have recognized the value of white space bands in wireless communication. Various proposals, including IEEE 802.11af, IEEE 802.22 and those from the White Spaces Coalition, have advocated using white spaces left by the termination of analog TV to provide wireless broadband Internet access. Some company from industry has designed device intended to use these available channels as a "white-spaces device" (WSD), such as Ubiquiti SR serials products. These devices are designed to detect the presence of existing but unused areas of airwaves, such as those reserved for analog television, and utilize these unused airwaves to transmit signals for data traffic. Such technology is predicted to improve the availability of broadband Internet service, especially in rural areas.

White space band not only provide more bandwidth for wireless communication, but also bring the diversity in transmission range. Our algorithms and frameworks try to combine white space bands and WiFi bands in link communication and network deployment improvement.

2.2. Gateworks Platform

The off the shelf platform we use for our measurments is the GW2358. GW2358 is a member of the Gateworks Cambria Single Board Computer family. The GW2358 meets the requirements for enterprise and residential network applications. This single board computer consists of an Intel IXP435 XScale operating at 667MHz, 128Mbytes of DDRII-400 DRAM, and 32Mbytes of Flash. Peripherals include four Type III Mini-PCI sockets, two 10/100 Base-TX Ethernet ports with IEC-6100-4 ESD and EFT protection, two USB Host ports, and Compact Flash socket. Additional features include digital I/O, serial EEPROM, real time clock with battery backup, system monitor to track operating temperature and input voltage, RS232 serial port for management and debug, and watchdog timer. The GW2358 also supports GPS and RS485 serial port as ordering options. Power is applied through a dedicated connector or through either Ethernet connector with the unused signal pairs in a passive power over Ethernet architecture. An opensource software OpenWrt board support package is included for Linux operating systems.

We use Gateworks platform with Ubnt radios to perform 802.11 multiband measurements for both indoor and in-field. It helps to collect the SNR, throughput and packet information for the post process.

2.3. Rohde & Schwarz FSH8 Spectrum Analyzer

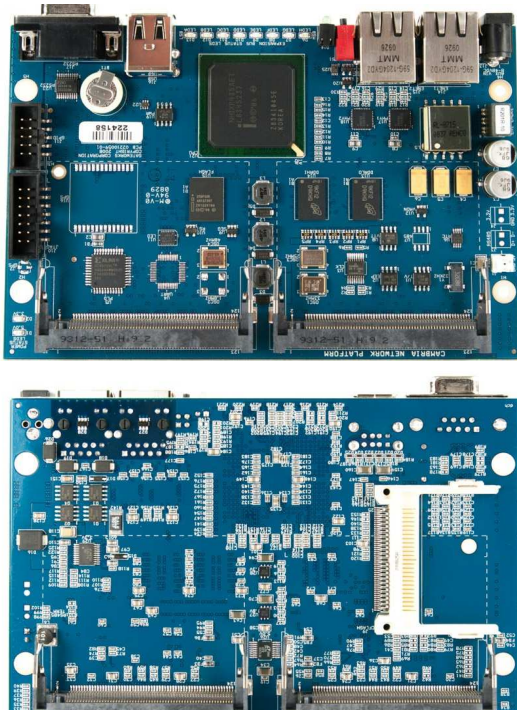

Figure 2.1. The Gateworks GW2358 off-shelf Platform.

Figure 2.2. Rohde & Schwarz FSH 8 Spectrum Analyzer.

The R&S FSH 8 spectrum analyzer is portable and designed for use in the field. Its low weight, its simple, well-conceived operation concept and the large number of measurement functions make it an indispensable tool for anyone who needs an efficient measuring instrument for outdoor work.

FSH 8 could sense the signal in the air from 9 KHz to 8 GHz. The spectrum analyzer could sense both 802.11 signals and non-802.11 signal in the air. Through the time stamp, we could merge data from Gateworks platform and FSH8 platform to perform our algorithms and frameworks.

2.4. Mesh Network Deployment

Wireless Mesh Network is the infrastructure to provide wireless access for clients. Wireless mesh network is made up of radio nodes organized in a mesh topology. Each

node forwards messages on behalf of the other nodes. The nodes connected to clients are counted as the access tier, the nodes to relay data traffic to wired networks are backhual tier. For access tier, the nodes need to cover the service area and provide enough capacity for the clients in the service area. The backhual tier need to have high efficient connection to the wired network. We analyze the mesh network deployment in multiband scenario, and propose our solution for access and backhual network deployment.

Chapter 3

Vehicular Link Spectrum Adapatation

In this section, we first formulate the multiband adaptation problem in vehicular wireless links and introduce the set of information we use to make band decisions, which we refer to as context information. We then propose two machine-learning-based multiband adaptation algorithms for vehicular channels. For comparison, we also propose two baseline adaptation methods based on existing solutions which consider historical and instantaneous information independently.

3.1. Link Adaptation Problem Formulation

Consider a system with n frequency bands, represented by an index set $\{1, 2, \ldots, n\}$. The objective is to select the optimal band, b_{best}, to transmit at each time instant that maximizes a desired objective function such as throughput. The throughput r_i on band i depends on several factors such as received signal power P_R^i, noise power P_N^i, the channel busy time B^i, the velocity of the transmitter, v_{tx}, the velocity of the receiver, v_{rx}, and location information which depends on each algorithm and will be specified in the algorithm section. The aforementioned set of all information used to make multiband decisions composes the users context. This relationship is represented in general as $r_i = f(P_R^i, P_N^i, B^i, v_{tx}, v_{rx}$,context information per algorithm). The objective can be stated as:

$$b_{best} = \arg\max_i r_i \tag{3.1}$$

The framework differentiates interference from other nodes using the same technology (via the busy time B^i) and other technologies (via the noise level P_N^i). For

instance, an 802.11 node can decode the packets of other 802.11 nodes but can only sense instantaneous noise levels from ZigBee/Bluetooth nodes. Decoding the packets can provide increased knowledge such as data rate and packet size to determine the duration of the channel use. We can exploit the long-term behavior by using historical performance data for the collected context information (*e.g.*, v_{tx}, v_{rx}, B^i, P_N^i, P_R^i) [38].

To represent the utilization level of the channel, we define *busy time*, B, as the percentage of time when the channel is occupied by all competing sources $x_j (j = 1, 2, 3, ...)$ other than the intended transmitter y. For 802.11-based transmissions, the busy time on band i is defined as:

$$B^i = \frac{\sum_j \sum_k \frac{L_k^{x_j}}{R_k^{x_j}}}{\sum_k \frac{L_k^y}{R_k^y} + \sum_j \sum_k \frac{L_k^{x_j}}{R_k^{x_j}} + S\sigma} \tag{3.2}$$

where $L_k^{x_j}$ and $R_k^{x_j}$ represent the packet length in bits and data rate at which that packet is transmitted, for external sources x_j; S and σ are the number of idle slots and slot duration, respectively. When considering the activity level of non-802.11 users (*e.g.*, the bands currently licensed to TV), we use the received signal level from non-802.11 interfering sources P_N^i on band i directly as an input to our algorithms.

3.2. Multiband Adaptation Algorithms

In order to evaluate the proposed multiband adaptation algorithms, we construct two baseline methods: (i.) We search for the most commonly selected band as the best band in the historical data and choose it as the final band decision. (ii.) For each band, we build a lookup table for throughput T_{ideal} in an idealized channel given the $RSSI$ and obtain the best band according to following:

$$\max_i T_{ideal}^i \times (1 - B^i), \tag{3.3}$$

The throughput T_{ideal} is measured with an Azimuth ACE-MX channel emulator [3]. The details of the system setup and data collection are discussed in Section **??**.

Machine learning has been used as an important tool in wireless communications [28]. When a user enters an area, the machine learning algorithm can learn from the historical data and select the potential optimal band given the input, *e.g.*, P_R^i, v and P_N^i. We propose two multiband adaptation algorithms based on two machine learning methods: k-nearest neighbor (KNN) and decision trees.

Location-based Look-up Algorithm. KNN is a machine learning method based on searching for the closest training data points in the feature space and various modified versions have been applied successfully for classification [64]. In the *Location-based Look-up Algorithm*, we search for the closest neighbors of a testing point by using each parameter one by one in the input set. The *Location-based Look-up Algorithm* additionally involves geographic information for band selection other than received signal power P_R^i, noise power P_N^i, the activity/occupancy level B^i, the velocity of the transmitter, v_{tx}. The performance of the selected training data points is averaged to generate an estimate of the performance at each band. Then the band with the highest throughput performance is selected as b_{best}.

For the *Location-based Look-up Algorithm*, context information involves the location g (GPS latitude and longitude), v, P_R^i, P_N^i and B^i. To make a band prediction, we have four look-up blocks to reduce the training data points which are similar to the testing data point. First, we search for the historical data which is closest to the testing data based on GPS location. If the number of found historical data points is less than a predefined threshold, θ_{AArea}, we increase the distance range (the actual threshold is discussed in Section **??**). Then, based on the filtered historical data, we collect θ_{AArea} data points which are closest to P_R^i, where θ_{AArea} is the threshold of the number of collected data points. A similar process is repeated based on P_N^i and

v, respectively. After deciding the final data set, we average the throughput of data points at each band. This algorithm's key steps are shown in Algorithm 3.1.

Region-based Decision Tree Algorithm. Decision trees are a widely-used machine learning algorithm due to their low complexity and stable performance [17]. A decision tree can model the relationship in the training data between the context information and the optimal band as a set of tree-like deduction structures. Before implementing the training process, we prepare a training set including a group of training data points of $\{v_{tx}, v_{rx}, P_R^1, ..., P_R^n, B^1, ..., B^n, P_N^1, ..., P_N^n, b_{best}\}$ based on the collected measurements. We obtain b_{best} by comparing the throughput performance of all available bands and selecting the band with the highest throughput. We choose the C4.5 algorithm to generate our decision tree [27], a widely-used algorithm based on the information entropy gain.

At each intermediate node in the decision tree, the learning algorithm calculates the information entropy gain of splitting the remaining training data points based on each parameter in the input set, *e.g.*, P_R^i, v or P_N^i. Then, it compares and selects the parameter with the highest entropy gain to decide the test condition at each intermediate node until all training data points are classified. The leaf nodes indicate the optimal band for prediction in our application. Then, the trained decision structure is integrated into the transmitter protocol stack. With the collected context information, the decision structure can suggest the band with the best throughput performance.

The relationship between the context information and the best band could differ at different locations because of diverse propagation environment characteristics. To reduce the heterogeneity of training data from different locations, we split the vehicular route into several regions and implement the training process based on the historical data collected in each region. Then, the trained decision structure is in-

Algorithm 3.1 Location-based Look-up Algorithm

Input:

g: Location information of multiband node

θ_{Area}: Threshold of a location

θ_{RSSI}: Threshold of RSSI

$\theta_{Velocity}$: Threshold of velocity

θ_{AArea}: Threshold of data amount for a location

θ_{ARSSI}: Threshold of data amount for RSSI

$\theta_{ANon802.11SI}$: Threshold of data amount for non-802.11 interference

$\theta_{AVelocity}$: Threshold of data amount for velocity

$D^i \in \{D^1, D^2, \ldots, D^n\}$: Historical look-up data

Output:

b_{best}: Optimal transmission band

1: **for** $i <= n$ **do**

2: Initialize $Data_{Location}, Data_{RSSI}, Data_{Velocity}$ to zero matrix;

3: **while** $Amount(Data_{Location,i}) < \theta_{AArea}$ **do**

4: $Data_{Location,i} \leftarrow f_{Lookup}(D^i, g, \theta_{Area})$: Find data in D^i whose distance less than θ_{Area};

5: $\theta_{Area} = \theta_{Area} \times 1.1$;

6: **end while**

7: **while** $Amount(Data_{RSSI,i}) < \theta_{ARSSI}$ **do**

8: $Data_{RSSI,i} \leftarrow f_{Look-up}(D_{Location,i}, P_R^i, \theta_{RSSI})$: Find data in $D_{Location}$ the RSSI similar to P_R^i in range θ_{RSSI};

9: $\theta_{RSSI} = \theta_{RSSI} \times 1.1$;

10: **end while**

11: **while** $Amount(Data_{P_N,i}) < \theta_{ANon802.11SI}$ **do**

12: $Data_{RSSI,i} \leftarrow f_{Look-up}(D_{Location,i}, P_N^i, \theta_{RSSI})$: Find data in $D_{Location}$ the RSSI similar to P_N^i in range θ_{RSSI};

13: $\theta_{ANon802.11SI} = \theta_{ANon802.11SI} \times 1.1$;

14: **end while**

15: **while** $Amount(Data_{Velocity,i}) < \theta_{AVelocity}$ **do**

16: $Data_{Velocity,i} \leftarrow f_{Lookup}(D_{RSSI,i}, v, \theta_{Velocity})$: Find data in D_{RSSI} the RSSI similar to v in range θ_{RSSI};

17: $\theta_{Velocity} = \theta_{Velocity} \times 1.1$;

tegrated in our system for multiband adaptation in each region. The granularity of regional division is one parameter that affects the training set as well as the performance of the resulting decision tree. We evaluate the granularity of these divisions in Section 3.3.

3.3. Experiments for Multiband Algorithms

To study these algorithms, we have developed indoor and in-field experiments on a Linux-based 802.11 testbed [4]. The platform includes a Gateworks 2358 motherboard with Ubiquiti XR radios (XR9 at 900 MHz, XR2 at 2.4 GHz, XR5 at 5.2 GHz) and a DoodleLabs DL475 radio at 450 MHz [2, 6]. We use an Azimuth ACE-MX channel emulator for controllable propagation and fading characteristics with a broad range of industry-standard channel models from 450 MHz to 5.9 GHz [3].

3.3.1. In-lab Experiments for Radio Characterization

To establish an SNR-to-throughput relationship for the *SNR-based Throughput Look-up Algorithm*, we use an experimental setup where two wireless nodes communicate across repeatable emulated channels generated by the channel emulator (Figure 3.1). For a given band and card, we measure the throughput of a fully-backlogged UDP flow using the *iperf* traffic generator. We use constant attenuation over an idealized channel condition and repeat the experiment to produce various RSSI values. Despite the same physical and media access control layers of the radios, there are slight differences in the throughput achieved per radio at the same attenuation level. Thus, we normalize these throughput values to have the same maximum throughput across radio types.

3.3.2. Experimental Design for In-field Data Collection

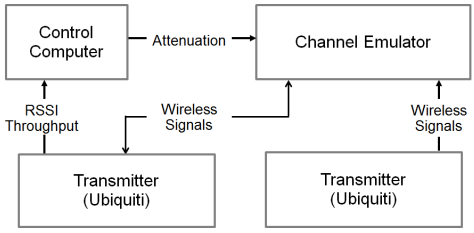

Figure 3.1. Experimental setup for channel emulator.

We now describe the in-field experimental design to obtain a data set for evaluating our multiband algorithms. Two Gateworks boards, each containing the aforementioned four radios, are installed on two cars. One node is always the receiver and at a fixed location. The other node is always the transmitter and travels around the block of a public park as shown in Figure 3.2. One loop of the route will be used as a unit of training in the next section.

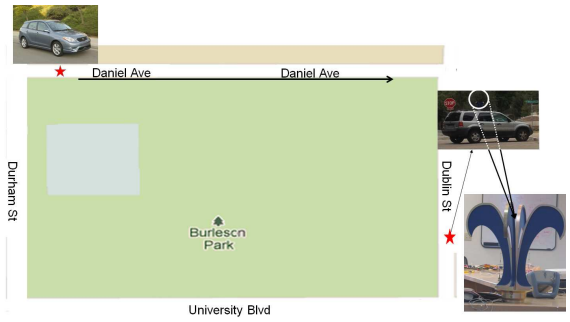

Figure 3.2. In-field Experimental Setup.

During each loop, the transmitter sends a fully-backlogged UDP flow using *iperf* on each of the four radios simultaneously. To focus on band selection and ensure the greatest range, we disable autorate and use a fixed data rate of 6 Mbps. The receiver continually performs a *tcpdump* of all received 802.11 packets [32]. Additionally, a QH 400 Quad Ridge Horn Antenna (shown in Figure 3.2) is connected to a Rhode & Schwarz FSH8 mobile spectrum analyzer at the receiver to monitor spectral activity. Then, based on the time stamps, we remove 802.11 packets from the spectral trace

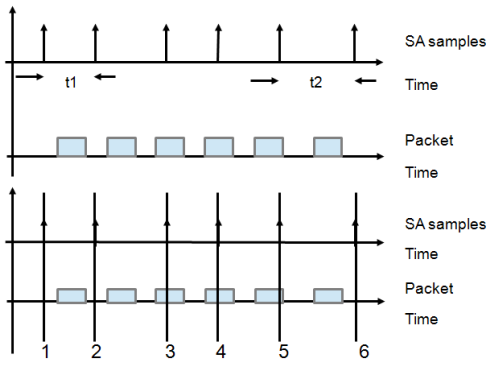

Figure 3.3. Spectrum Analyzer Data Processing.

so that only non-802.11 interference will contribute to P_N^i.

Figure 3.3 shows how we obtain the non-802.11 interference, P_N^i. We expunge the spectrum analyzer (SA) samples which overlap in time with the dumped 802.11 packets, such as packets 3, 4, and 5. Then, the reported interference value will not contain the received power from 802.11 packets, which have already been considered via the busy time, B.

The in-field data is processed offline where data from all instruments involved is synchronized based on the GPS time stamps. As discussed in Section 3.3.1, the throughput of each radio is normalized based upon emulator experiments to account for any manufacturing differences.

3.4. Performance Analysis of Algorithms

We now evaluate our proposed algorithms with the experimental setup described in Sections 3.3.1 and 3.3.2. The metrics of *Accuracy* and *Throughput Gap* are used in the evaluation. We consider each second of the in-field trace and observe the frequency band that had the highest throughput. The *Accuracy* is defined as the percentage of best band predictions that match the observed optimal band, where a prediction is made each second. Conversely, the *Throughput Gap* is defined as the difference

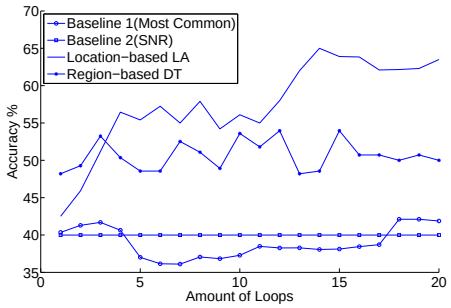

Figure 3.4. Accuracy of the four multiband algorithms.

between the throughput observed on the optimal band and the throughput achieved by the predicted best band over the throughput of the observed optimal band. In the situation where the optimal band is not chosen, the throughput could be close between the chosen and optimal bands, meaning that the incorrect band choice did not result in a large throughput loss. Thus, the *Throughput Gap* metric captures the severity of the incorrect choice.

Since the *SNR-based Throughput Look-up Algorithm* requires only emulator-based training, the *Accuracy* and *Throughput Gap* can be calculated for all loops of the in-field trace. However, the *Location-based Look-up Algorithm* and *Region-based Decision Tree Algorithm* require in-field training. Thus, the data set must be divided into a training set and testing set for evaluation.

In Figure 3.4, we show the aforementioned *Accuracy* of the four multiband algorithms in selecting the band with the highest throughput. The x-axis represents the number of loops around the block of the mobile transmitter (shown in Figure 3.2) that will be used by the machine-learning-based algorithms. We use the same training and testing set to compare the *Location-based Look-up Algorithm* and *Region-based Decision Tree Algorithm*. From the results, we observe the following:

- At each loop, the first baseline algorithm, *Most Commonly-Selected Band*, uses the band with the greatest long-term average of the percentage of time that

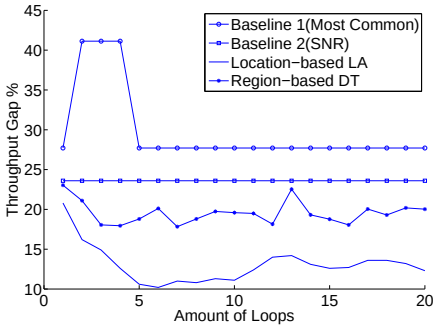

Figure 3.5. Throughput Gap of the four multiband algorithms.

band yields the highest throughput over the previous loops. The accuracy ranges from 36.1% to 42.9%.

- The second baseline algorithm, *SNR-based Throughput Look-up*, maintains 39.2% across all the loops since it relies only on emulator-based training.

- The *Region-based Decision Tree Algorithm* has an accuracy ranging from 48.2% to 54.0% but contains many dips due to the relationship between the context information and the distribution of the best band choice changing on a loop-by-loop basis. Additional training data slightly improves the decision structure overall but primarily induces additional noise in the training process.

- The *Location-based Look-up Algorithm* begins with an accuracy of 42.5% but improves the most out of any algorithm to finish with an accuracy 62.5% with the highest accuracy of 65.0% occurring after loop 14. Additional in-field training loops are likely to further improve the multiband selection accuracy.

Figure 3.5, depicts the *Throughput Gap* of the four algorithms we evaluated and shows the following.

- The *Most Commonly-Selected Band Algorithm* has two different modes of throughput gap based upon which band has the highest long-term percentage. For loops

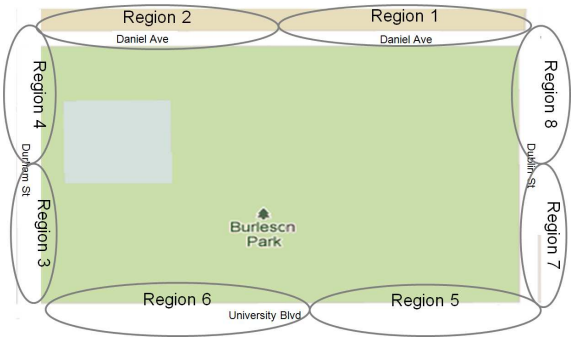

Figure 3.6. Spatially splitting experimental area into 8 regions.

2-4, the choice is 5.8 GHz, which has a gap of 41.1% using the test set. For all other loops, the choice is 2.4 GHz, which has a gap of 27.7%.

- The *SNR-based Throughput Look-up Algorithm* shows a baseline performance of 23.6% for the throughput gap.
- The *Region-based Decision Tree Algorithm* benefits from additional training, going from a throughput gap of 23.0% to 20.0%. Spatial and temporal changes to context information bring dips to the curve as discussed earlier.
- Finally, the *Location-based Look-up Algorithm* takes only 6 loops of training to reach its lowest value of 10.2% in terms of throughput gap. From loops 1 to 20, the throughput gap goes from 20.8% to 12.3%, which might still be improved upon with additional training.

We now consider the effect of further sub-dividing in-field experimental testing data into regions for our *Location-based Look-up Algorithm* and *Region-Based Decision Tree Algorithm*. To do so, we divide the loop around the park into eight regions as shown in Figure 3.6, which has two competing effects: (i.) Smaller regions allow similar experimental data to be used in the training process, potentially improving the decision structure. (ii.) For a given training set, dividing it into regions reduces the number of training points for the machine learning algorithms, potentially weakening

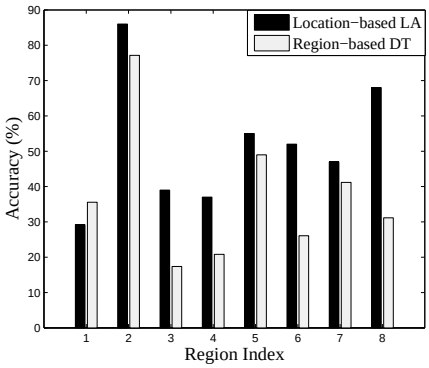

Figure 3.7. Accuracy when dividing training set into 8 regions.

the decision structure. In Figure 3.7, we observe the *Accuracy* of the eight regions for both algorithms.

- In all but Region 1, the *Location-based Look-up Algorithm* has better performance than *Region-based Decision Tree Algorithm*. The improved accuracy of the former algorithm can be attributed to its ability to distinguish each point's relative distance to the middle of the region For the *Region-based Decision Tree Algorithm* to capture such a notion, the regions would have to be further subdivided, increasing the number of trees and reducing the training set per tree.

- For this training set, the reduction in training data caused by the regional divisions had a net loss on the performance of the *Region-based Decision Tree Algorithm*. However, if the training set was much larger for a given area, the net effect of regional divisions could be positive.

3.5. Related Work

Cognitive Radio could be a powerful tool for the utility of the Spectrum Opportunity [28]. Analog TV bands will be released for wireless communication brings opportunity to combine current wireless bands and new available bands for performance improvement employing Cognitive Radio methods [34].

A bunch of work has been done on radio-scene analysis and channel identification for utility of channel adaptation dating back to Simon Haykin [28]. Some work of Multi-bands/Multi-channels in cognitive radios focus on optimize performance, such as avoiding frequency diversity [43]. In [55] an opportunistic algorithm is introduced to balance the cost of spectrum sensing, channel switching and the gain of these activities.

Our work is motivated by prospective releasing band used for TV now and exploit the comparison across all the available bands in the future. It is an extension of multi-channel adaptation. Most of the published research focus on the stopping rules of spectrum sensing [54, 55]. In contrast, we use the data and framework to classify the performance across different bands based on the parameters we get from the context information.

3.6. Summary

In this paper, we investigated multiband adaptation to leverage the propagation and context for vehicular applications. We did so by proposing two machine-learning-based schemes and compared their performance against two baseline schemes. In our experimental analysis, we evaluated the performance of these algorithms in the field on an off-the-shelf platform. Experimental results demonstrate that the proposed algorithms can achieve up to 49.3% greater throughput than the baseline algorithms with an accuracy up to 65%. In future work, we will study the impact that multiple diverse environments have on the training as well as evaluate the optimal use of multiple, diverse radios in unison.

Chapter 4

Spectrum Adapatation in Access Tier Network

In this chapter, we illustrate the challenges of band selection in wireless network deployments and formulate the problem of band selection in wireless network deployments jointly using WiFi and white space bands. Further, we present a measurement-driven framework for estimating the access point number to serve the traffic demand of a given population.

4.1. White Space Opportunity and Challenge

Wireless propagation refers to the signal loss characteristics when wireless signals are transmitted through the wireless medium. The strength of the received signal depends on both the line-of-sight path (or lack thereof) and multiple other paths that result from reflection, diffraction, and scattering from obstacles [13]. The widely-used Friis equation characterizes the received signal power P_r in terms of transmit power P_t, transmitter gain G_t, receiver gain G_r, wavelength λ of the carrier frequency, distance R from transmitter to receiver, and path loss exponent n according to [23]:

$$P_r = P_t + G_t + G_r + 10n \log_{10} \left(\frac{\lambda}{4\pi R} \right) \tag{4.1}$$

Here, n varies according to the aforementioned environmental factors with a value ranging from two to five in typical outdoor settings [47].

Despite sufficient levels of received signal, interference can cause channels to be unusable (e.g., due to high levels of packet loss) or unavailable (e.g., due to primary users in cognitive radios [28]). Prior work has worked to reduce interference levels via

gateway deployment, channel assignment, and routing [29, 59]. The interference of a wireless network could be divided into two categories according to the interfering source: *(i)* intra-network interference, caused by nodes in the same network, and *(ii)* inter-network interference, caused by nodes or devices outside of the network. Most of the existing works try to reduce the intra-network interference without regard to the inter-network interference [57]. However, the existence of inter-network interference becomes an important problem when considering the availability of white space bands. While theoretical models which describe inter-network interference exist, accurately characterizing a particular region must be done empirically.

When wireless devices operate in WiFi bands, the channel separation is relatively small (e.g., 5 MHz for the 2.4 GHz band). As a result, many works assume that the propagation characteristics across channels are similar. However, with the large frequency differences between WiFi and white space bands (e.g., multiple GHz), propagation becomes a key factor in the deployment of wireless networks with both bands. Here, a frequency band is defined as a group of channels which have little frequency separation, meaning they have similar propagation characteristics. In this work, we consider the diverse propagation and activity characteristics for four total frequency bands: 450 MHz, 800 MHz, 2.4 GHz, and 5.2 GHz. We refer to the two former frequency bands as white space bands and the two latter frequency bands as WiFi bands. The differences in propagation and spectrum utilization create opportunities for the joint use of white space and WiFi bands in wireless access networks according to the environmental characteristics (e.g., urban or rural and downtown or residential) of the deployment location.

Typically, the deployment of wireless access networks is subject to coverage and capacity constraints for a given region. Coverage is defined with respect to the ability of clients to connect to access points within their service area. We use a coverage

constraint ratio of 95% in this work for a target area [51]. Capacity is defined with respect to the ability of a network to serve the traffic demand of clients. Spatial reuse allows improved capacity but increases the cost of deploying a network by increasing the total number of access points required. Hence, for densely-populated areas, the greatest level of spatial reuse possible is often desired. In contrast, sparsely-populated rural areas have lower traffic demand per unit area. Thus, aggregating this demand with the use of lower frequencies via white space bands could be highly effective in reducing the total number of access points required to achieve similar coverage and capacity constraints. Moreover, since less TV channels tend to be occupied in sparsely-populated areas [8], a larger number of white space bands can be leveraged in these areas.

4.2. Model and Problem Formulation

As opposed to previous works such as [59, 63, 57], this paper focuses on reducing the inter-network interference for various population densities for wireless access networks which jointly employ WiFi and white space bands. We propose a measurement-driven framework to estimate the number of access points required for serving the traffic demand of a certain area. We assume an access point has a limited number of radios which operate on any channel of a fixed number of channels with the same antenna gain. Each radio on an access point operates with a classic protocol model [26]. We further assume that there is a given take rate and traffic demand for a given population (as specified in Section 4.3).

For spectrum utility and resulting channel availability, we use a long-term measurement for each band. We define the percentage of sensing samples (S_θ) above an interference threshold (θ) over the total samples (S) in a time unit as the activity

level (A) of inter-network interference:

$$A = \frac{S_\theta}{S_a} \tag{4.2}$$

The capacity of a clean channel is denoted by C. With the protocol model, the capacity of a channel with inter-network interference C_r could be represented as the remaining free time of the channel capacity according to:

$$C_r = C * (1 - \bar{A}) \tag{4.3}$$

A network deployment should ideally provide network capacity equal to the demand of the service area to maintain the capacity constraint. The demand of a service area could be calculated as the summation of individual demands all over the service area $D_a = \sum_{p \in P} D_p$. Since household demand for the Internet has been previously characterized [53], D_a could represent the population distribution f and service area k as $D_a = \sum_{f \in F, k \in K} \bar{D_p} * f * k$. The capacity constraint could be represented with an access point set M according to:

$$\sum_{m \in M} C_r^m \geq \sum_{f \in F, k \in K} \bar{D_p} * f * k \tag{4.4}$$

At the same time, the wireless network must additionally satisfy the coverage constraint in the service area where the access points provide connectivity for client devices. Generally, a coverage of 95% is acceptable for wireless access networks [51].

In a joint white space and WiFi scenario, the activity level varies according to various interfering sources and the propagation characteristics induced by the environmental characteristics of the service area. A simple method with the least number of access points to cover an area is to use multiple orthogonal lower-frequency channels. However, the FCC limits white space band availability for data networks in most metropolitan areas in the United States [7]. Moreover, the number of channels in each band is limited. Too many lower-frequency channels will cause high levels of

Algorithm 4.1 Multiband Access Point Estimation (MAPE)

Input:

A: Measured Activity Level

F: Population Distribution

C: Clean Channel Capacity

n: Path Loss Exponent

B: Available Frequency Bands

M: Area to be Covered

1: Split M in to different type, calculate the traffic demand density f

2: Calculate in-field channel capacity C_r as $C(1 - A)$

3: Get the propagation coverage area radius R_p from the Friis model based on n, B, F

4: Calculate the QoS coverage radius R_{QoS} of a multiband access point that satisfies the demands of the area

5: The coverage radius of a multiband access point is $MinR_p, R_{QoS}$

6: Apply a regular-hexagonal deployment to get the number of access points for serving given area M

Output:

The number of access points

intra-network interference for the network, which is out of our scope in this work. We assume that the cost of the network is proportional to the number of access points required for a given user demand (i.e., due to the cost of hardware and installation). Therefore, given a geographical region for a new network deployment, we build a measurement-driven framework called Multiband Access Point Estimation (MAPE) to compute the required number of access points.

In the space domain, the advantage of higher-frequency channels is the spatial reuse, while the lower-frequency channels provide greater levels of coverage. Generally, higher frequencies are more appropriate for populated areas, and lower fre-

quencies are more appropriate for sparse areas. The temporal variation of spectrum utilization differs across bands. For an Internet service provider, the service quality which maps to the capacity constraint must be satisfied. Given a metropolitan area, the population distribution can be found according to census data [9]. Then, we can estimate the capacity demand of each type of area with the assumption that users will exhibit average demand. According to the population distribution, we split the area into different types, which compose the spatial input. Then, we use the measured activity level as the temporal input. We have an average channel capacity of each band according to the activity level. With the received signal strength threshold, the Quality-of-Service-constrained coverage area of different types per channel, and the spatial reuse distance can be directly computed. Then, the maximum area an access point could cover can be calculated as the minimal area of the QoS-based coverage area and propagation coverage. Then, the transmission power is adjusted to fulfill the coverage restriction subject to the FCC regulations for maximum-allowable transmit power. A classic regular-hexagonal deployment process is employed to place the access points.

4.3. Experiment and Analysis

To evaluate the spectrum utility from in-field measurements, we perform experiments with an off-the-shelf wireless platform and mobile spectrum analyzer. According to the measured data, we apply our MAPE framework to analyze the role of white space and WiFi bands in the total access points required for a given deployment area and user demand.

4.3.1. Experiment Design

We employ a Linux-based 802.11 testbed, which includes a Gateworks 2358 board with Ubiquiti XR radios (XR9 at 900 MHz, XR2 at 2.4 GHz, XR5 at 5.2 GHz) and a DoodleLabs DL475 radio at 450 MHz. We develop shell scripts which utilize tcpdump to enable the testbed to work as a sniffer, recording all 802.11 packets. However, since the Gateworks platform only updates its estimate of received signal strength upon the reception of a new packet (and not all relevant channel activity is 802.11 based), we employ a spectrum analyzer to form a notion of inter-network interference with finer granularity. Hence, we also use a Rohde & Schwarz FSH8 portable spectrum works from 100 KHz to 8 GHz. The portable spectrum analyzer is controlled by a Python script on a laptop to measure the received signal strength.

To the best of our knowledge, there is no readily available mobile, multiband antenna from 450 MHz to 5.2 GHz on the market. Thus, we use a 700-MHz mobile antenna to perform in-field measurements. We then normalize the mobile antenna performance across bands with indoor experimentation. To do so, we use a Universal Software Radio Peripheral (USRP) N210 to generate signals at 450 MHz, 800 MHz, and 2.4 GHz. We feed the USRP signals directly to a spectrum analyzer and adjust the configuration of USRP to make the received signal strength the same as the 5.2 GHz signal from Gateworks 2358 with a XR5 radio. Then, we connect the signal source to a fixed multiband antenna (QT 400 Quad Ridge Horn Antenna) and measure the received signal at a fixed distance with the 700 MHz antenna and antennas for different bands to obtain the antenna loss for each band. We adjust the received signal strength collected via the 700-MHz mobile antenna according to the normalization.

Our experimental platform is shown in Figure 4.1. The mobile spectrum analyzer records 32 samples per second on each band under test with appropriate time stamps. The Gateworks sniffer platform also records all the received WiFi packets according to their time stamps. The duplicate samples in WiFi bands from spectrum analyzer and

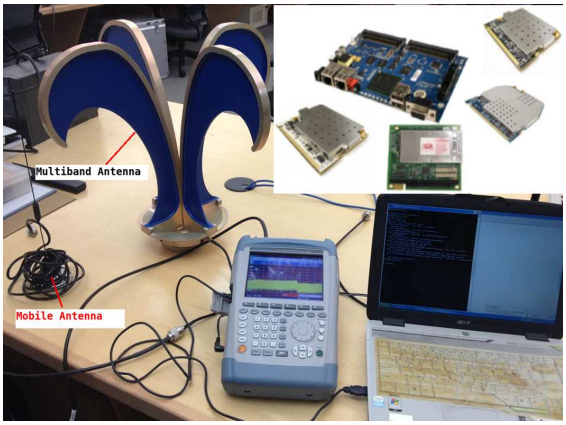

Figure 4.1. Multiband Measurement Platform

Gateworks are deleted according overlapping time stamps. Accordingly, we calculate the activity level in WiFi bands. The activity level of white space bands is calculated solely based upon the spectrum analyzer measurements.

Figure 4.2 depicts a map of the available white space channels with markers where we performed measurements in North Texas. To be representative of a broad range of community types, we consider populations of approximately 25 times one another according to the 2010 U.S. Census, Millsap (500), Weatherford (25K), and Dallas (1.25 M). We have collected measurements at multiple types of locations in Dallas, including a downtown area, a residential area, and a university campus. In Weatherford and Millsap, we monitor wireless activities in three locations for 45 continuous minutes on a weekday in downtown, residential, and non-residential areas. Then, we post-process the data to calculate the activity level of each band in each location. First, we parse the SNR from the data logs via Perl scripts. Second, we merge the data from the two platforms according to their respective time stamps and calculate the activity level of each band across these locations. The activity level is then included in our framework as input parameter.

4.3.2. Results and Analysis

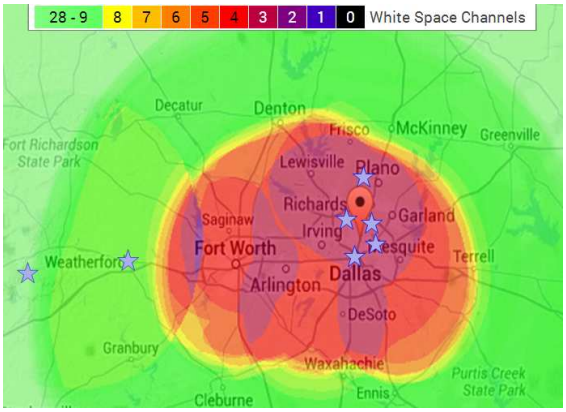

Figure 4.2. White Space Channels in DFW Metropolitan and Surrounding Areas.

In this subsection, we discuss our measurements results and leverage our MAPE framework to analyze the influence of white space channels across areas with different population densities. As an initial experiment, we perform a drive test from Dallas to Weatherford with cruise control set to 60 MPH while on the highway. The result of the in-field spectrum drive test is shown in Figure 4.3 according to the location and time of the measurement. The measured activity via RSSI of 450 MHz is high in downtown Dallas and Fort Worth but has less signal activity in the urban and rural area between these city centers. The low activity detected in the WiFi bands is due to the distance from the highway being typically larger than the propagation range of predominantly indoor wireless routers. Our initial in-field measurement matches the FCC restrictions (shown in Figure 4.2) with less channels available translating to greater spectrum utilization by TV stations. The drive test also shows that the spectrum utilization is roughly proportional to the population density in Figure 4.3. We use the measurements collected at more fixed locations as marked on the map for the activity level calculation.

The activity level calculated with our measurements are shown in Table 4.1. Dallas, the city with the greatest population in North Texas, has the highest activity level in most of the measured bands, especially at 450 MHz. The Dallas urban measure-

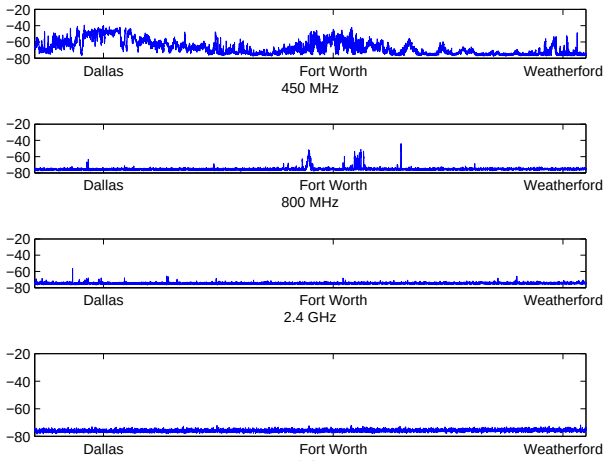

Figure 4.3. Spectrum Activity in DFW Metropolitan and Surrounding Areas.

Bands	Dallas			Weatherford			
Area Type	Downtown	Residential	Suburban	Downtown	Residential	Sparse	Downtown
450 MHz	24.37	25.83	23.77	6.05	12.50	14.03	7.00
800 MHz	4.40	16.49	4.77	5.22	5.07	4.43	3.87
2.4 GHz	15.87	34.95	2.60	2.03	2.03	2.77	2.07
5.2 GHz	19.70	35.46	1.53	1.93	1.93	1.33	1.27

Table 4.1. Activity Level in Multiple Locations

ments are taken from the SMU campus, two neighborhoods, and a densely-populated suburb (Plano). Our measurements indicate that 2.4 GHz has a higher activity level in urban area than the measured downtown area. Most schools and their neighborhoods are covered by WiFi, which contributes to the high activity level at 2.4 GHz and 5.2 GHz. In Weatherford, all the bands have lower activity levels than in Dallas. A peculiarity in the measurements can be seen by the sparse area in Weatherford having more activity than the other regions for 450 MHz. This can be explained due to the measurement location being on the East of Weatherford (closer to Fort Worth, which has a population of approximately 750k). Millsap is a typical sparse rural area with approximately 500 total residents. The activity levels across all the bands are lower than in Dallas and Weatherford. In the 450 MHz band, the activity level decreases much faster than in other bands in Dallas and Weatherford.

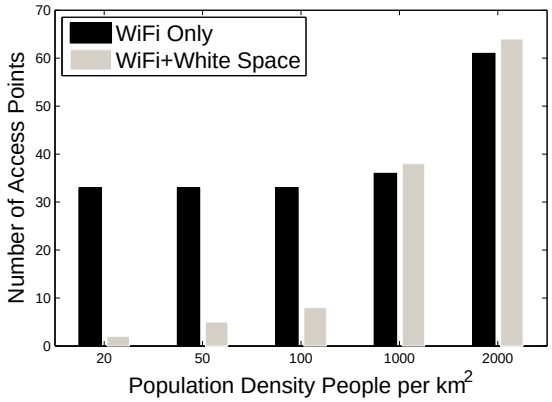

Figure 4.4. Number of Access Points Needed for a 13 km x13 km Area.

We use the measurement-based activity levels shown in Table 4.1 in our framework presented in Algorithm 4.1. We specifically use the Millsap sparse area, Millsap downtown, Weatherford residential, Dallas residential, and Dallas downtown measurements as inputs of activity level for a given population density. We then calculate the number of access points for covering a 13 km $\times$ 13 km area, varying the population density. The output is shown in Figure 4.4.

In the calculation, we set the demand requested per user as 2 Mbps with the population density of 20, 50, 100, 1000, and 2000 users per square kilometer. We assume 30 % of the residents will use this service (i.e., the take rate is 30 %), the maximum transmit power is 30 dBm, and a path loss exponent of 3.5 [38]. From Equation 5.1, we see that the propagation range is proportional to the wavelength with 450 MHz having a propagation range of 11.6 times that of 5.2 GHz. We adopt an 802.11n maximum data rate of 600 Mbps. For the WiFi+White Space scenario, we use 3 channels in each of the 450 MHz, 2.4 GHz and 5.2 GHz bands. For the WiFi Only scenario, we assume 6 channel in the 2.4-GHz band, and 3 channels in the 5.2-GHz band since 2.4 GHz has larger propagation range than 5.2 GHz. Each of these scenarios have the same channels in total (9). As shown in Figure 4.4, with the same number of channels, WiFi+White Space reduces the number of access points by

1650% compared to the WiFi Only scenario in the 20 people per square km scenario, 660% in the 50 people per square km, and 412.5% in the 100 people per square km scenario. The large propagation range of the white space bands is approximately 10 times that of the WiFi bands, creating an opportunity for greater coverage. However, as the population density increases, due to the capacity constraint of servicing users in the area, the lower-frequency white space bands lose their advantage of larger communication range due to the reduction in achievable spatial reuse. At the same time, the activities of other signal sources, such as TV stations in downtown areas, reduce the capacity of white space bands. As a result, the WiFi+White Space scenario performs worse than the WiFi Only scenario. If we were to count the intra-network interference (out of scope), the situation could become even worse. Moreover, FCC has stricter policies on white spaces in urban areas. Fewer channels are available in these areas, which makes WiFi a better option for dense areas.

To understand the influence of band combinations on network deployments, we calculate the number of access points in the area when selecting 500 people per square km with a downtown Weatherford spectrum utilization and 1500 people per square km with a residential Dallas spectrum utilization. We assume the total number of channels is 12. We use the same setup as the previous experiment.

In Table 4.2, we compare the number of access points with 12 channels through all the possible combinations of bands. Since purchasing and deploying access points is the primary cost of a wireless infrastructure, to simplify the calculation, we only count the number of access points as the network's cost. When all the channels are in the same band, as the frequency goes up, more access points are needed to serve the area due to the limited propagation range. However, 450 MHz does not outperform 800 MHz with a single band at both the 500 and 1500 people per square km cases because 450 MHz channels have larger measured activity levels. White space band channels

No. of Bands	Bands Combination (Hz)	No. of AP	
		500 ppl/km^2	1500 ppl/km^2
1	450 M	12	35
	800 M	10	30
	2.4 GHz	33	37
	5.2 G	193	193
2	450 M,800 M	11	32
	450 M,2.4 G	23	36
	450 M,5.2 G	23	69
	800 M,2.4 G	20	33
	800 M,5.2 G	20	59
	2.4 G,5.2 G	33	73
3	450 M,800 M,2.4 G	16	33
	450 M,800 M,5.2 G	16	48
	450 M,2.4 G,5.2 G	33	53
	800 M,2.4 G,5.2 G	30	49
4	450 M,800 M,2.4 G,5.2 G	21	44

Table 4.2. Channel Combinations for 500 and 1500 Population Density Scenarios

outperform WiFi bands by up to 1830% in the single band case with 500 people per square km, but with 1,500 people per square km, the cost reduction decreases to only 543%. We now distribute an equal number of channels to two-band combinations and run the experiments with the same population densities and spectrum utilization. The results shows the white space band combination (450 and 800 MHz) performs better than WiFi only (2.4 and 5.2 GHz) by 200% and 128% with the people per square km of 500 and 1,500, respectively. In fact, the white space only scenario (450 and 800 MHz) has almost the same performance as the scenarios with one white band and one WiFi band (450 MHz and 2.4 GHz; 800 MHz and 2.4 GHz) with 1,500 people per square km. However, with 500 people per square km, the white space only scenario is much better than any other two-band combination. White space channels provide

up to 87.5% cost reduction in three-band combination scenarios with 500 people per square km, and up to 33.3% with 1,500 people per square km. With four bands, the number of access points required does not reduce using white space bands.

From Figure 4.4 and Table 4.2, we show that as the population density increases, the reduction in number of access points required to meet the same demand diminishes. Note that a more optimal allocation of channels in different bands could offer further cost reductions. We further show that as population and spectrum utilization increase, at some point, the performance of white space only scenario could be the same as a combination of white space and WiFi bands.

4.4. Related Work

Prior work in wireless network deployment has focused extensively on solving gateway placement, channel assignment, and routing problems to reduce the interference generated inside the network [29, 44, 11]. Unfortunately, few works in network deployment notice the interference across networks. Some cognitive radio works discuss this inter-network interference, but most of them focus on point-to-point communication other than taking a network-wide view [18].

With new FCC regulations on the use of white space bands, there are two factors to consider with such bands: large propagation range and existing inter-network interference from TV stations and other devices such as microphones [5, 21, 15]. Prior work does not specifically study the benefits of jointly using white space and WiFi bands in the deployment of wireless access networks [12]. Additionally, prior work related to white spaces target opportunistic media access. However, the application of white spaces across diverse population densities has not been fully explored.

Finally, some works discuss the propagation variation in both WiFi bands and white space bands. For example, Robinson et al. models the propagation variation

at the same band in terrain domain [51]. Another work proposes a database-driven framework for designing a white space network with database of primary user (TV station) locations and channel occupation [41]. However, these works do not jointly study the influence of white space and WiFi bands on network deployment according to their resulting propagation variation and spectrum utilization.

4.5. Summary

In this paper, we jointly considered the use of WiFi and white space bands for deploying wireless access networks across a broad range of population densities. To consider network deployment costs, we proposed a Multiband Access Point Estimation framework to find the number of access points required in a given region. We then performed spectrum utilization measurements in the DFW metropolitan and surrounding areas to drive our framework and find the influence of white spaces on network costs in these representative areas. Through extensive analysis across varying population density and channel combinations across bands, we show that white space bands can reduce the number of access points by 1650% and 660% in rural and sparse urban areas, respectively. However, the same cost savings are not achieved in dense urban and downtown type area. Finally, we investigate different band combinations in two population densities to show that greater access to white space channels have greater total savings of mesh nodes when the total number of channels used in the network is fixed (i.e., given a total number of allowable WiFi and white space channels). As the population and spectrum utilization increase, the cost savings of white space bands diminish to the point that WiFi-only channel combinations can be optimal. In the future, we will consider the heterogeneous access points and traffic demand scenarios in wireless network deployments.

Chapter 5

Spectrum Adapatation in Backhual Tier Network

In this chapter, we formulate the problem of how to optimally use WiFi and white space bands in concert when deploying wireless mesh networks. We first describe our system model and illustrate the challenges of such a WhiteMesh architecture. We then discuss how to evaluate WhiteMesh networks and the corresponding goal of both the optimization framework and the heuristic algorithm that we propose in the following section. Finally, we present our integer linear programming model used to address the problem and the performance of the algorithms.

5.1. WhiteMesh Network Architecture

Wireless propagation is the behavior of the signal loss characteristics when wireless signals are transmitted from a transmitter to receiver. The strength of the receiving signal depends on both the line-of-sight path (or lack thereof) and multiple other paths that are a result of reflection, diffraction, and scattering from obstacles in the environment [13]. The widely-used Friis equation characterizes the power of the received signal P_r in terms of the power P_t and gain G_t of the transmitting signal, gain of the receiver G_r, wavelength λ of the carrier frequency, distance R from transmitter to receiver, and path loss exponent n according to [23]:

$$P_r = P_t + G_t + G_r + 10n \log_{10} \left(\frac{\lambda}{4\pi R} \right) \tag{5.1}$$

Here, the path loss exponent n changes according to the aforementioned environmental factors and ranges from 2 to 5 in typical outdoor settings [47].

A common assumption in works that use many WiFi channels is that the propagation characteristics of one channel is similar to another, since the channel separation is relatively small (e.g., 5 MHz for the 2.4 GHz band). Many works which rely on such an assumption have focused on the allocation of multiple WiFi channels with multiple radios in multihop wireless networks [57]. Here, a frequency band is defined as a group of channels which have similar propagation characteristics. In this work, we consider the diverse propagation characteristics for four frequency bands: 450 MHz, 800 MHz, 2.4 GHz, and 5.8 GHz. We refer to the two former frequency bands as white space (WS) bands, whereas we refer to the two latter frequency bands as WiFi bands.

Wireless mesh networks are a particular type of multihop wireless network that are typically considered to have at least two tiers [19]: *(i)* an access tier, where client traffic is aggregated to and from mesh nodes, and *(ii)* a multihop backhaul tier for connecting all mesh nodes to the Internet through gateway nodes. In this work, we focus on how to optimally allocate white space and WiFi bands on a finite set of radios per mesh node along the backhaul tier, since we assume that client devices will use WiFi (due to the economies of scale). In each of the WhiteMesh topologies studied in Section **??**, a sufficient number of orthogonal WiFi channels remain for the access tier to connect to clients using additional radios co-located on the mesh nodes.

Due to the broadcast nature of the wireless medium, greater levels of propagation induce higher levels of interference. Thus, in sparsely-populated rural areas, the lower frequencies of the white space bands might be a more appropriate choice for multihop paths to gateways having reduced hop count. However, as the population and demand scales up (e.g., for urban regions), the reduced spatial reuse and greater levels of interference of white space bands might detract from the overall deployment strategy. In such urban areas, select links of greater distance might be the most

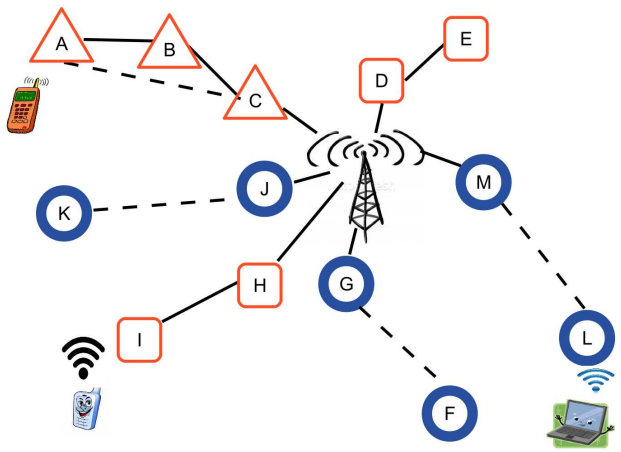

Figure 5.1. Example WhiteMesh topology with different mesh-node shapes representing different frequency band choices per link.

appropriate choice for white space bands, especially since the number of available channels is often inversely proportional to the population (due to the existence of greater TV channels).

Figure 5.1 depicts an example where mesh node A could connect to mesh node C through B at 2.4 GHz, or directly connect to C at 450 MHz. If 2.4 GHz were used, link D, E might be able to reuse 2.4 GHz if they are out of the interference range. However, if link A, C used 450 MHz, a lower hop count would result for the path, but lower levels of spatial reuse also result (e.g., for link D, E). While the issues of propagation, interference, and spatial reuse are simple to understand, the joint use of white space and WiFi bands to form optimal WhiteMesh topologies is challenge.

5.2. Model and Problem Formulation

Our model is similar to prior multi-channel models [59, 63, 57]. However, in these models, different channels have the same communication range D_c and interference range D_r. While these works would attempt to maximize throughput in a multihop network topology by an optimal channel assignment for a given set of radios, we

hypothesize that using radios with a greater diversity in propagation could yield overall network performance gains. Therefore, for a given set of radios, we allow the channel choices to come from multiple frequency bands (i.e., multiband channel assignment, which also includes multiple channels in the same band). To simplify the analysis, we assume the channel capacity of each band is equal. In practice, we could easily calculate the proportional ratio of channels in each band according to their bandwidth. We assume that the locations of mesh nodes and gateway nodes are given and all mesh nodes have the same transmit power, channel bandwidth, and antenna gain. Each mesh node operates with a classic protocol model [26].

A mesh network could be represented by a unidirectional graph $G = (V, E)$, where V is the set of mesh nodes, and E is the set of all possible physical links in the network. If the received signal (according to Eq. 5.1) between two mesh nodes i, j for a given frequency band (from the set of all bands B) is greater than a communication-range threshold, then a data link exists and belongs to the set L with a fixed, non-zero capacity γ according to the protocol model. Correspondingly, a connectivity graph C is formed for each band in B such that $C = (V, L, B)$. If the received signal for a given band is above an interference-range threshold, then contention occurs between nodes. We extend the conflict matrix in [59] according to different interference per band according to $F = (E_{i,j}, I_{Set}, B)$, where $E_{i,j}$ represents the link and I_{Set} includes all the links are physically inside the interference range D_r when operating on each band b.

Therefore, the problem we address is: to choose the connectivity graph C which maximizes the served user demand according to the throughput achieved through the gateway (defined below). A key challenge is that selecting the optimal channels from the set B leads to a conflict graph F which cannot be known *a priori*. Previous works have proposed a coloring, cluster-independent set, mixed linear integer methodology

for a single band b [39, 42, 59]. However, these works do not address a reduction in hop count or an increase in spatial reuse for a set of diverse bands B. In particular, the goal of a network backhaul layer is to maximize the amount of mesh user demand served, which can be measured by the total goodput achieved through the gateways. Thus, to evaluate the performance of the multiband channel assignment, we use a performance metric of gateway goodput X, where:

$$X = \sum_{w \in W, v \in V} T(w, v) \tag{5.2}$$

Since the bottleneck of mesh network capacity has been shown to be the gateway's wireless connections [52], gateway goodput considers all incoming and outgoing wireless traffic T onto the Internet. We describe the exact calculation of gateway goodput in Section 5.4 and consider gateway placement outside the scope of this work.

5.2.1. Mixed Integer Linear Programming Formulation

We now present a mixed integer, linear programming formulation for optimizing gateway goodput when selecting channels for WhiteMesh topologies across diverse bands. We assume that the set of available mesh nodes (V), gateways (W), and available bands (B) are given. The communication links and conflict graph are given as parameters.

Sets:
- V set of nodes
- B set of bands

Parameters:

$\gamma^b_{i,j}$	$(i,j) \in V, b \in B$	capacity of link i,j on band b
$I^b_{ij,lm}$	$(i,j,l,m) \in V, b \in B$	Interference of link (i,j) on band b
W_i	$i \in V$ *binary*	Gateways in network
D_{di}	$i \in V$	Downlink demand of node i
D_{ui}	$i \in V$	Uplink demand of node i

We define the time share to represent the percentage of time a single link transmits according to $\alpha^b_{i,j}$ for link i,j in band b. Two terms are defined for uplink and downlink flows:

Variables:

$0 \leq \alpha^b_{ij} \leq 1$	$b \in B, (i,j) \in N$	Time share of link (i,j) on band b
$0 \leq uy^b_{i,j,k}$	$(i,j,k) \in V, b \in B$	Uplink flow of node k on link (i,j) at band b
$0 \leq dy^b_{i,j,k}$	$(i,j,k) \in N, b \in B$	Downlink flow of node k on link (i,j) at band b

Our objective is to maximize the gateway goodput (X).

Objective:

$$Max \sum_i \sum_j \sum_k \sum_b (uy^b_{i,j,k} + dy^b_{j,i,k}) \; When \; w_j = 1 \tag{5.3}$$

The connectivity, uplink, and downlink constraints are:

Connectivity Constraints:

$$\alpha^b_{i,j} + \alpha^b_{j,i} + \sum_l \sum_m (\alpha^b_{l,m} \cdot I^b_{ij,lm}) \leq 1, i \neq j \tag{5.4}$$

$$\sum_i uy^b_{i,j,k} + \sum_i dy^b_{i,j,k} \leq r^b_{j,k} \cdot \alpha^b_{j,k} \tag{5.5}$$

Uplink Constraints:

$$\sum_k \sum_b uy^b_{i,i,k} \leq D_{ui} \; when \; w_k = 0, i \neq k \tag{5.6}$$

$$uy^b_{i,j,k} = 0 w_k = 1 \tag{5.7}$$

$$\sum_i \sum_b uy^b_{i,j,k} = \sum_m \sum_b uy^b_{j,m,k} \; when \; w_k = 0, i \neq k \tag{5.8}$$

$$uy^b_{i,j,i} = 0 \tag{5.9}$$

Downlink Constraints:

$$\sum_j \sum_b dy^b_{i,j,i} \leq D_{di} \; when \; w_i = 0 \tag{5.10}$$

$$dy^l_{i,j,k} = 0 \; when \; w_k = 1 \tag{5.11}$$

$$\sum_j \sum_b dy^b_{i,j,k} = \sum_m \sum_b dy^b_{j,m,k}, \; when \; w_k = 0, i \neq k \tag{5.12}$$

$$dy^b_{i,i,j} = 0 \tag{5.13}$$

In the ILP, (5.4) represents the summation of the incoming and outgoing wireless time share and the interfering links' wireless time share, which should all be less than 1. Constraint (5.5) represents the incoming and outgoing wireless traffic, which should be less than the link capacity for link i, j. Uplink constraints (5.6) and (5.7) represent that the summation of any wireless flow i, j should be less than the demand of node k. Constraints (5.8) and (5.9) are used to restrict the sum of all incoming data flows for a given mesh node k to be equal to the sum of all outgoing flows. Downlink constraints (5.10) and (5.11) are similar to (5.6) and (5.7) but in the downlink direction. Similarly, constraints (5.12) and (5.13) are downlink versions of (5.8) and (5.9).

Linear programs which attempt to solve channel assignment and routing in multihop wireless networks have been proved to be NP hard [59, 63]. The model jointly considers channel assignment factors and provides the methodology to achieve the upper bound on gateway goodput. Once we have a particular channel assignment $A_{i,j}^{k}$, we can modify the objective function, parameters, and constraints to find the maximum satisfied demand in the network.

5.3. Path Analysis with Diverse Propagation

In this section, we discuss the influence of diverse propagation characteristics of the wide range of carrier frequencies of white space and WiFi bands. We then introduce our heuristic algorithm for channel assignment in WhiteMesh networks.

5.3.1. Path Interference Induced on the Network

In WhiteMesh networks, multihop paths can be intermixed with WiFi and white space bands. To consider which combination is better, we consider which band choices reduce the number of hops along a path and the aggregate level of interference that hop-by-hop path choices have on the network (i.e., Path Interference induced on the Network).

Due to random access, mesh nodes closer to the gateway generally achieve greater levels of throughput at sufficiently high offered loads. To combat such starvation effects, we treat each flow with equal priority in the network when assigning channels. In particular, all nodes along a particular path have equal time shares for contending links (i.e., intra-path interference). At the beginning of a particular channel assignment, we assume that h mesh nodes are demanding traffic from each hop of an h-hop path to the gateway. If each link along the path uses orthogonal channels, then each link could be active simultaneously. Consider that if each node along the path had

traffic demand T_d, the bottleneck link along the path would be closest to the gateway. Then, the total traffic along the path $h \cdot T_d$ must be less than the bottleneck link's capacity γ. In such a scenario, the h-hop mesh node would achieve the minimum served demand, which we call the network efficiency. In general, the active time per link for an h-hop mesh node can be represented by $1, \frac{h-1}{h}, \frac{h-2}{h} \cdots \frac{1}{h}$. The summation of all active times for each mesh node along the path is considered the intra-path network cost.

Considering only intra-path interference, using lower carrier frequencies allows a reduction in hop count and increase in the network efficiency of each mesh node along the h-hop path. However, a lower carrier frequency will induce greater interference to other paths to the gateway (i.e., inter-path interference). Fig. 5.1 depicts such an example where links in different bands are represented by circles for 450 MHz, rectangles for 2.4 GHz, and triangles for the nodes which can choose between the two. Nodes A and C could be connected through two 2.4-GHz links or a single 450-MHz link. With 2.4 GHz, the interfering distance will be less than using 450 MHz. For example, only link D, E will suffer from interference, whereas H, I would not. However, with 450 MHz, link A, C would interfere with links F, G, M, L, and K, J. At each time unit, the number of links interfering with the active links along a path would be the inter-path network cost.

When an h-hop flow is transmitted to a destination node, it prevents activity on a number of links in the same band via the protocol model. The active time on a single link can be noted as $\frac{T}{\gamma_h}$. An interfering link from the conflict matrix F counts as I_h per unit time and contributes to the network cost in terms of: $\frac{hT}{\gamma_1} \cdot I_1 + \frac{(h-1)T}{\gamma_2} \cdot I_2 \cdots \frac{T}{\gamma_h} \cdot I_h$. Then, the traffic transmitted in a unit of network cost for the h-hop node is:

$$E_\eta = \frac{T}{\sum_{i \in h} \frac{(h-i+1) \cdot T}{\gamma_i} \cdot I_i} \tag{5.14}$$

Using network efficiency, the equation simplifies to:

$$E_\eta = \frac{\gamma}{\sum_{i \in h}(h - i + 1) \cdot I_i} \tag{5.15}$$

The network efficiency is the amount of traffic that could be offered on a path per unit time. With multiple channels from the same band, I_i will not change due to the common communication range. With multiple bands, I_i depends on the band choice. This network efficiency jointly considers hop count and interference. We define the Path Interference induced on the Network (PIN) as the denominator of Eq. 5.15, which represents the sum of all interfering links in the network by a given path. We use PIN to assign channels across WiFi and white space bands. To determine when the lower carrier frequency will be better than two or more hops at a higher carrier frequency, we consider the average interference $\bar{I}$ of a given path at the higher frequency. The problem could be formulated as:

$$\frac{\gamma}{\frac{h(h-1)}{2} \cdot \bar{I} + I_x} \geq \frac{\gamma}{\frac{h(h+1)}{2} \cdot \bar{I}} \tag{5.16}$$

Here, when $I_x \leq 2 \cdot h\bar{I}$, a lower-frequency link could be better than two higher-frequency hops along the same path. I_x is also a function of hop count in Eq. 5.15. When the hop count is lower, the threshold would be more strict since the interference would have a greater effect on gateway goodput.

5.3.2. Band-based Path Selection (BPS) Algorithm

We design a Band-based Path Selection (BPS) algorithm (described in Alg. 5.1) which first chooses the mesh node that has the largest physical distance from the gateway nodes. When a path is constructed for the mesh node with the greatest distance, all subsequent mesh nodes along the path are also connected to the gateway. The central concept behind the BPS algorithm is to improve the worst mesh node performance in a path. For large-scale mesh networks, it is impractical to traverse

all the paths with different combination of bands from a mesh node to any gateway node. However, based on the discussion in Section 5.3.1, if two paths have the same number of used bands along those paths, then the path with the least hops is likely to have the greatest performance and is chosen. Similarly, if two path have the same path interference, we choose the path which has higher-frequency links for spatial reuse. Thus, the next step of the algorithm is to find the shortest path across band combinations.

Compared to the number of mesh nodes, the amount of channels N_B in different bands is small. The time complexity of calculating the combination is $O(2^{N_B})$. Finding the shortest path in Dijkstra algorithm will cost $O(N_E^2)$ according to [25], where N_E is the links in the network, and as a result, the total complexity would be $O(N_E^2 \cdot 2^{N_B})$. The algorithm would then calculate the PIN of the candidate path and select the path with the least interference induced on the network for the source mesh node. After a path is assigned, the algorithm updates the network's channel assignment with served nodes, activated links, and radio information. Then, we iteratively assign channels for all the mesh nodes in the network.

If all the nodes are connected ($N_E = \binom{n}{2}$ which is $O(N_V^2)$), then the complexity of assigning a channel for a mesh node is $O(N_E^2 \cdot 2^{N_B})$. Then, the complexity of assigning a mesh node is $O(N_V^4 \cdot 2^{N_B})$. To assign *all* the nodes in the network, the complexity would be $O(N_V^5 \cdot 2^{N_B})$.

5.4. Evaluation of WhiteMesh Channel Assignment

We now extensively evaluate our proposed heuristic algorithm against the upper bound formed by our integer linear program and versus prior channel assignment strategies. We introduce the topologies and metric calculation used in the analysis and present a set of results based of the linear program and heuristic algorithm.

5.4.1. Experimental Evaluation Setup

A key aspect of WhiteMesh networks is the diversity in propagation from the lowest white space channels (tens to hundreds of MHz) to the highest WiFi channels (multiple GHz). Thus, to evaluate the performance of our algorithms, we consider a wide range of propagation characteristics from four different frequency bands. For white space bands, we consider 450 and 800 MHz. For WiFi bands, we consider 2.4 and 5.8 GHz. With similar transmission power and antenna gain, the highest carrier frequency would have the shortest communication range. Hence, we set a communication-range threshold of -100 dBm, and normalize the communication range with the highest frequency of 5.8 GHz. In particular, the communication range of 450 MHz, 800 MHz, 2.4 GHz, and 5.8 GHz would be normalized to 12.8, 6.2, 2.4, and 1, respectively. The interference range is computed as twice that of the communication range [45]. We deploy static wireless mesh networks of n mesh nodes along a regular, rectangular grid with a normalized distance of 0.8 between rectangular edges. As a result, we have varying degrees of connectivity in the grid. The gateways are randomly-selected from one out of every six mesh nodes in the network. Unless otherwise, specified in the analysis, all four bands are used in the WhiteMesh topology studied.

The throughput achieved through the gateways is not only critical for network providers (e.g., cellular carriers charge fees for total bandwidth through towers), but also has been used by researchers to evaluate channel assignment [14]. As mentioned previously, the wireless capacity of gateway nodes has been shown to be the bottleneck in mesh networks [51]. Moreover, gateway goodput combines multiple factors, such as mesh node placement, gateway placement, routing, and channel assignment, the latter of which is the focus of our analysis and algorithms. For the purposes of our analysis, we specifically calculate the gateway goodput first introduced in Section 5.2

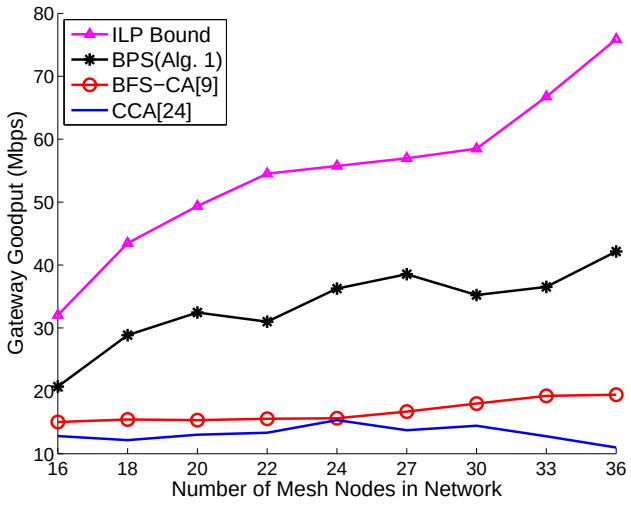

Figure 5.2. Average Population Distribution = 600 ppl/km^2

in the following way. Mesh nodes that have a one-hop path to the gateway nodes are the first ones served. Where there are nodes with the same hop count, the least interfering mesh nodes are chosen for channel assignment. Then, the demand of multihop mesh nodes are served until there is no remaining demand to be satisfied through any path.

We vary the average population distribution of the target area, assuming 10% of the residents will use our service. An individual would have a $100KB/s$ traffic demand on average. Then, we randomly assign the user distribution across the area and run the analysis of each case 20 times. We relax our ILP model to keep the link capacity constraints, given the demand of the mesh nodes as a parameter to achieve the maximum throughput at the gateways. The ILP Bound assumes the mesh nodes could connect to all the gateways if there is a path that exists to each gateway. However, we restrict a mesh node to only connect to one gateway in the network, and this represents the main difference from the ILP Bound to our heuristic algorithm.

5.4.2. Experimental Analysis of WhiteMesh Backhaul

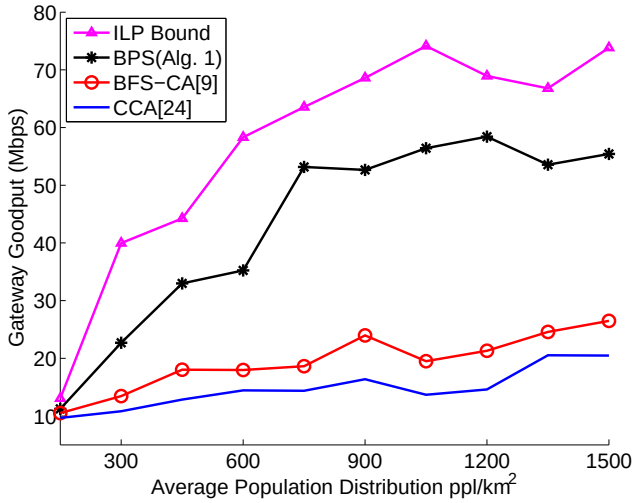

Figure 5.3. Varying Load, 30-Node Regular Grid

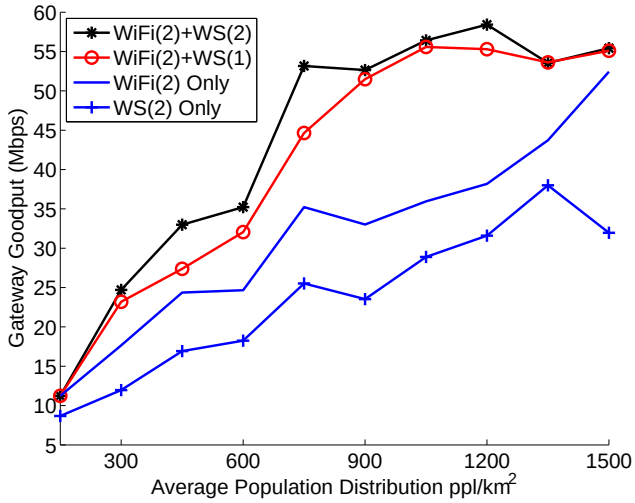

Figure 5.4. BPS (Alg. 1), Varying WS Availability

Bands/ Algorithms	WiFi Only	WS Only	WS & WiFi	WS & WiFi	WS & WiFi	WS & WiFi	WS & Multi-WiFi	WS & Multi-WiFi	Mu
WS (MHz)		450,800	450	800	450	800	450	800	
WiFi (GHz)	2.4, 5		2.4	2.4	5	5	2.4, 5	2.4, 5	
CCA [22]	3.1	7.3	8.2	8.1	8.3	7.8	8.7	9.3	
BFS-CA [44]	8.9	6.2	7.9	9.0	13.6	13.8	14.9	13.8	
BPS (Alg. 1)	22.2	18.2	28.4	25.0	30.9	25.8	32.0	33.5	

Table 5.1. Throughput achieved through Gateway nodes (Mbps) for various combinations of WiFi and Average Population Distribution = 600 ppl/km^2, Network Size = 30 mesh nodes).

Typically, clients and mesh nodes have diverse traffic patterns with the download direction dominating the total traffic demand (e.g., consider service agreements for cellular data or Internet connectivity). Hence, to simplify the analysis and scale the ILP Bound to larger network sizes, we remove the uplink constraints while maintaining the downlink constraints. We then randomly assign demand per mesh node with a maximum offered load as specified in Fig. **??** and Table 5.1. We repeat the process 20 times, averaging the results of each of the algorithms for the given network configuration.

In the first experiment, we consider different network sizes according to the number of mesh nodes in the aforementioned regular grid. In particular, we expect that as the network size grows, so too does the number of gateways, producing a greater total gateway goodput. Fig. 5.2 shows the total gateway goodput when the population distribution is 600 ppl/km^2 for the ILP formulation and the heuristic algorithms: *(i)* Common Channel Assignment (CCA) from [22], *(ii)* Breadth First Search Channel Assignment (BFS-CA) from [44], *(iv)* our algorithm BPS (Section 5.3.2). In CCA [22], two nodes will assign a channel for each other when there is a common free channel for both of the nodes. In BFS-CA [59], a node will search all the available one-hop connections then choose the one has the largest capacity for a new assignment. These two methods assume the one-hop connections are equal when there is no assignment on the channel. In BPS, we both consider and leverage propagation differences of diverse bands.

In Fig. 5.2, we observe dips in the curves for all algorithms, representing the randomly generated demand. The ILP Bound shows what could be expected, that an increasing number of gateways produce an increase in total gateway goodput. However, we observe that the other algorithms are not able to achieve such behavior for various reasons. CCA increases the average hop count the most, meaning that it

was unable to find shorter routes to new gateways. BFS-CA fails to increase the reach of the gateway by attempting to optimize the first hop from the gateway. Conversely, BPS alleviates the strain on these first-hop, bottleneck links, achieving up to 63% of the ILP Bound. The key difference of BPS to the ILP is that BPS only considers one path to a gateway node for each mesh node, whereas the ILP allows multiple paths to the gateways.

Next, we consider a different form of scalability in our analysis. Namely, we increase the average population distribution from 150 to 1,500 per km^2, while maintaining a 30-node regular grid topology. Fig. 5.3 shows that all of the algorithms are able to achieve comparable gateway goodput at 150 ppl/km^2. However, as the population distribution increases, the ILP and BPS diverge greatly from the remaining algorithms. Similar to Fig. 5.2, the wireless capacity around a gateway is quickly saturated if the algorithm is not focused on preserving that resource. Nonetheless, we do observe a leveling off at approximately 60 Mbps offered load due to a similar effect of the saturation of wireless capacity around the gateway node. For BPS, this saturation point at 60 Mbps has a gateway goodput from 1.5 to 3.2 times that of the remaining three algorithms, whereas the ILP Bound has between 2.7 and 4.18 times the gateway goodput. BPS has a performance of 75% of the ILP Bound, on average.

WhiteMesh networks will be deployed across a vast array of environments, from rural to urban areas. Each of these areas will have varying amounts of user demand in proportion to the population densities. However, since a greater number of TV stations exist in urban areas, the available white space bands are often inversely related to the population density. To capture these varying degrees of demand and white space availability we consider three likely scenarios and one final scenario for comparison purposes: *(i)* two WiFi bands (2.4 and 5.8 GHz) with two white space channels (450 and 800 MHz), *(ii)* two WiFi bands (2.4 and 5.8 GHz) with one white

space channel (450 MHz), *(iii)* two WiFi bands (2.4 and 5.8 GHz) without any white space channels, and *(iv)* two white space bands (450 and 800 MHz) with no WiFi bands (for comparison).

In Fig. 5.4, we consider the performance of BPS in the four aforementioned scenarios of varying white space availability with varying offered load from 1 to 10 Mbps, representing different population densities. A regular, 30-node grid is again used. Immediately, we observe that the WiFi-only scenario has greater gateway goodput than the white-space-only scenario. This is due to the lack of spatial reuse achieved by white spaces. Interestingly, however, the joint use of both white space and WiFi bands has significant gains over the single type of band scenarios (37% greater than WiFi and 85% over white space, on average). This can be explained in part because the joint use of WiFi and white space has more total bands to use. However, we will see in Table 5.1 that even with the same number of available bands (2), the combination of the two can achieve significant gains over scenarios with only WiFi or white space.

Table 5.1 describes the achieved gateway goodput for various combinations of WiFi and white space bands with a maximum offered load of 4 Mbps and a regular 30-node grid. The second reason for the gains in Fig. 5.4 with WiFi and white space is completely isolated in this scenario. Consider the case where we use a white space band of 450 MHz and a WiFi band of 5.8 GHz. With BPS and the same bandwidth, transmission power, and antenna gain, we achieve 30.9 Mbps of gateway goodput through jointly use of these bands, versus 22.2 Mbps with WiFi only or 18.2 Mbps for white space only with gains of 40% and 70%, respectively. If we have one channel in a white space band and one channel in a WiFi band, then we could use the advantage of WiFi for spatial reuse and white spaces to reduce the hop count. These two points become more critical at different points in the WhiteMesh topology. For the

sake of completeness, we present many other scenarios which could be interesting for WhiteMesh deployments.

5.5. Related Work

Optimization and Game Theory. Optimization frameworks based on linear programming have been used to determine the channel assignment in multihop wireless networks for given link bandwidths and route requests [59]. Since these formulations attempt to solve NP-hard problems, LP relaxation is commonly used to output network flows that potentially are not feasible channel assignments [57]. Game theory has also been used to guide distributed channel assignment and routing algorithms which attempt to balance the load of the network [45, 60]. In such a framework, nodes advertise their dynamically-changing costs to reach their associated gateway according to the residual bandwidth. If a node learns of a less expensive path to the current gateway or another gateway, the appropriate action is taken to construct such a path, but hysteresis must be carefully considered to avoid route flapping.

Multi-Channel, Multi-Radio Algorithms. Many works have studied the channel assignment problem in multihop wireless networks [33, 12, 46]. In addition, multiple radios have been used to improve the routing in multi-channel scenarios [22]. Still others have used static channel assignments where everything is known about the network parameters [58], which is in contrast to dynamic channel assignment where demand and interference are not known *a priori* [62, 44]. We have implemented such channel assignment algorithms (CCA from [22] and BFS-CA from [44]) and shown significant gains. Most importantly, all of the aforementioned works have not considered propagation differences of the diverse frequency bands of white space and WiFi, which we show are critical improving the performance of mesh networks.

White Space. To be used effectively, white space bands must ensure that available TV bands exist but no interference exists between microphones and other devices [15]. Since TV channels are fairly static in their channel assignment, databases have been used to account for white space channel availability (e.g., Microsoft's White Space Database [8]). In fact, Google has even visualized the licensed white space channels in US cities with an API for research and commercial use [7]. In contrast, we study the performance of mesh networks with a varying number of available white space channels at varying population densities, assuming such white space databases and mechanisms are in place.

5.6. Summary

In this paper, we exploited the joint use of WiFi and white space bands for improving the served user demand of wireless mesh networks. To do so, we used an integer programming model to find optimal WhiteMesh topologies. We then constructed a heuristic algorithms, Band-based Path Selection, to achieve similar performance with reduced complexity. Through extensive analysis across varying offered loads, network sizes, and white space channel availability, we show that our algorithms can achieve 3 to 6 times the served user demand versus previous multi-channel, multi-radio solutions, since we leverage diverse propagation characteristics offered by WiFi and white space bands. Moreover, we quantify the degree to which the joint use of these bands can improve the served user demand. Our BPS algorithm shows that WhiteMesh topologies can achieve up to 170% of the gateway goodput of similar WiFi- or white-space-only configurations.

Algorithm 5.1 Band-based Path Selection (BPS)

Input:

M: The set of mesh nodes

G: The set of gateway nodes

C: Communication graph of potential links among all nodes

I: Interference matrix of all potential links

B: Available frequency bands

Output:

CA: Channel Assignment of the Network

Rank mesh nodes according to physical distance from gateway
Initialize $S_{curr} = G$, $N_{srv} = \emptyset$, $N_{unsrv} = M$,$I_{active} = \emptyset$
while $N_{srv} =!M$ **do**
  Select node with largest distance to gateway
  Find the adjacency matrix across band combinations A_c
  for all $A_i \in A_c$ **do**
    Find the shortest path SP_i in mixed adjacency matrix A
    for all Link $l \in SP_i$, ordered from gateway to mesh node **do**
      Find the least interfering link
      If equally-interfering links, choose higher frequency
      Calculate the path interference of SP_i
    end for
    Store the shortest path SP_i as SP
  end for
  Assign the path in the network
  Update N_{srv}, N_{unsrv}
  Update I_{active} from I
end while
Output CA as the locally-optimal solution

Chapter 6

Proposed Work

Chapter 7

Conclusion

REFERENCES

[1] Metis: Mobile and wireless communications enablers for the twenty-twenty information society.

[2] Cambria gw2358-4 network platform. http://www.gateworks.com/, 2007.

[3] Aximuth ACE-MIMO Channel Emulator. http://www.azimuthsystems.com, Mar. 2011.

[4] Openwrt wireless freedom. https://openwrt.org/, Dec. 2011.

[5] Fcc white space. `http://www.fcc.gov/topic/white-space`, 2012.

[6] Ubiquiti xtremerange series of radio. http://www.ubnt.com/, 2012.

[7] Google spectrum database. `http://goo.gl/NnIFXQ`, 2013.

[8] Microsoft research white space database. `http://whitespaces.cloudapp.net/Default.aspx`, 2013.

[9] People and households. `http://www.census.gov/people/`, 2014.

[10] Afanasyev, M., Chen, T., Voelker, G., and Snoeren, A. Analysis of a mixed-use urban WiFi network: When metropolitan becomes neapolitan. In *ACM IMC* (2008).

[11] Akyildiz, I. F., Lee, W.-Y., Vuran, M. C., and Mohanty, S. Next generation/dynamic spectrum access/cognitive radio wireless networks: a survey. *Computer Networks 50*, 13 (2006), 2127–2159.

[12] Akyildiz, I. F., Wang, X., and Wang, W. Wireless mesh networks: a survey. *Computer networks 47*, 4 (2005), 445–487.

[13] Andersen, J. B., Rappaport, T. S., and Yoshida, S. Propagation measurements and models for wireless communications channels. *IEEE Communications Magazine 33*, 1 (1995), 42–49.

[14] Avallone, S., and Akyildiz, I. F. A channel assignment algorithm for multi-radio wireless mesh networks. *Computer Communications 31*, 7 (2008), 1343–1353.

[15] Bahl, P., Chandra, R., Moscibroda, T., Murty, R., and Welsh, M. White space networking with WiFi like connectivity. *ACM SIGCOMM 39*, 4 (2009), 27–38.

[16] Balanis, C. A. *Antenna theory: analysis and design.* John Wiley & Sons, 2012.

[17] Banfield, R., Hall, L., Bowyer, K., Kegelmeyer, W., et al. A comparison of decision tree ensemble creation techniques. *IEEE Trans on Pattern Analysis and Machine Intelligence 29*, 1 (2007), 173.

[18] Cabric, D., Mishra, S., and Brodersen, R. Implementation issues in spectrum sensing for cognitive radios. In *Signals, Systems and Computers, 2004. Conference Record of the Thirty-Eighth Asilomar Conference on* (2004), vol. 1, Ieee, pp. 772–776.

[19] Camp, J., Robinson, J., Steger, C., and Knightly, E. Measurement driven deployment of a two-tier urban mesh access network. In *ACM MobiSys* (2006).

[20] Cheng, J. Philadelphia's municipal WiFi network to go dark. `http://arstechnica.com/gadgets/2008/05/philadelphias-municipal-wifi-network-to-go-dark`, 2008.

[21] Cui, P., Liu, H., He, J., Altintas, O., Vuyyuru, R., Rajan, D., and Camp, J. Leveraging diverse propagation and context for multi-modal vehicular applications. In *IEEE WiVeC* (2013).

[22] Draves, R., Padhye, J., and Zill, B. Routing in multi-radio, multi-hop wireless mesh networks. In *ACM MobiCom* (2004).

[23] Friis, H. T. A note on a simple transmission formula. 254–256.

[24] Ghasemi, A., and Sousa, E. Spectrum sensing in cognitive radio networks: requirements, challenges and design trade-offs. *Communications Magazine, IEEE 46*, 4 (2008), 32–39.

[25] Golden, B. Shortest-path algorithms: A comparison. *Operations Research* (1976), 1164–1168.

[26] Gupta, P., and Kumar, P. R. The capacity of wireless networks. *IEEE Trans. on Information Theory 46*, 2 (2000), 388–404.

[27] Hall, M., Frank, E., Holmes, G., Pfahringer, B., Reutemann, P., and Witten, I. The weka data mining software: an update. *ACM SIGKDD Explorations Newsletter 11*, 1 (2009), 10–18.

[28] Haykin, S. Cognitive radio: brain-empowered wireless communications. *Selected Areas in Communications, IEEE Journal on 23*, 2 (2005), 201–220.

[29] He, B., Xie, B., and Agrawal, D. P. Optimizing deployment of internet gateway in wireless mesh networks. *Computer Communications 31*, 7 (2008), 1259–1275.

[30] Hossain, E., Chow, G., Leung, V., McLeod, R., Mišić, J., Wong, V., and Yang, O. Vehicular telematics over heterogeneous wireless networks: A survey. *Computer Communications 33*, 7 (2010), 775–793.

[31] Inc., C. Fcc certifies carlson wireless technologies tv white space radio. `http://www.carlsonwireless.com/rural-connect-press-release.html`, 2014.

[32] Jacobson, V., Leres, C., and McCanne, S. The tcpdump manual page. *Lawrence Berkeley Laboratory, Berkeley, CA* (1989).

[33] Jain, K., Padhye, J., Padmanabhan, V. N., and Qiu, L. Impact of interference on multi-hop wireless network performance. *Wireless networks 11*, 4 (2005), 471–487.

[34] Kanodia, V., Sabharwal, A., and Knightly, E. MOAR: A multi-channel opportunistic auto-rate media access protocol for ad hoc networks. In *Broadnets* (San Jose, CA, October 2004).

[35] Karrer, R., Sabharwal, A., and Knightly, E. Enabling large-scale wireless broadband: the case for TAPs. In *HotNets-II* (2003).

[36] Kim, S., Bertoni, H., and Stern, M. Pulse propagation characteristics at 2.4 ghz inside buildings. *Vehicular Technology, IEEE Transactions on 45*, 3 (1996), 579–592.

[37] Marina, M. K., Das, S. R., and Subramanian, A. P. A topology control approach for utilizing multiple channels in multi-radio wireless mesh networks. *Computer Networks 54*, 2 (2010), 241–256.

[38] Meikle, R., and Camp, J. A global measurement study of context-based propagation and user mobility. In *Proceedings of the 4th ACM international workshop on Hot topics in planet-scale measurement* (2012), ACM, pp. 21–26.

[39] Mishra, A., Banerjee, S., and Arbaugh, W. Weighted coloring based channel assignment for WLANs. *ACM SIGMOBILE MCCR 9*, 3 (2005), 19–31.

[40] Mo, J., So, H., and Walrand, J. Comparison of multi-channel mac protocols. In *Proceedings of the 8th ACM international symposium on Modeling, analysis and simulation of wireless and mobile systems* (2005), ACM, pp. 209–218.

[41] Murty, R., Chandra, R., Moscibroda, T., and Bahl, P. Senseless: A database-driven white spaces network. *Mobile Computing, IEEE Transactions on 11*, 2 (2012), 189–203.

[42] Peng, Y., Yu, Y., Guo, L., Jiang, D., and Gai, Q. An efficient joint channel assignment and QoS routing protocol for ieee 802.11 multi-radio multi-channel wireless mesh networks. *Journal of Network and Computer Applications* (2012).

[43] Rahul, H., Edalat, F., Katabi, D., and Sodini, C. Frequency-aware rate adaptation and mac protocols. In *Proceedings of the 15th annual international conference on Mobile computing and networking* (2009), ACM, pp. 193–204.

[44] Ramachandran, K. N., Belding-Royer, E. M., Almeroth, K. C., and Buddhikot, M. M. Interference-aware channel assignment in multi-radio wireless mesh networks. In *IEEE INFOCOM* (2006).

[45] Raniwala, A., and Chiueh, T. Architecture and algorithms for an IEEE 802.11-based multi-channel wireless mesh network. In *IEEE INFOCOM* (2005).

[46] Raniwala, A., Gopalan, K., and Chiueh, T.-c. Centralized channel assignment and routing algorithms for multi-channel wireless mesh networks. *ACM SIGMOBILE MCCR 8*, 2 (2004), 50–65.

[47] Rappaport, T. *Wireless Communications, Principles & Practice*. Prentice Hall, 1996.

[48] Rayanchu, S., Shrivastava, V., Banerjee, S., and Chandra, R. Fluid: improving throughputs in enterprise wireless lans through flexible channelization. In *Proceedings of the 17th annual international conference on Mobile computing and networking* (2011), ACM, pp. 1–12.

[49] Raychaudhuri, D., and Jing, X. A spectrum etiquette protocol for efficient coordination of radio devices in unlicensed bands. In *Personal, Indoor and Mobile Radio Communications, 2003. PIMRC 2003. 14th IEEE Proceedings on* (2003), vol. 1, IEEE, pp. 172–176.

[50] Reardon, M. EarthLink pays 5 million to delay houston Wi-Fi buildout. `http://news.cnet.com/8301-10784\_3-9768759-7.html`, 2007.

[51] Robinson, J., Singh, M., Swaminathan, R., and Knightly, E. Deploying mesh nodes under non-uniform propagation. In *IEEE INFOCOM* (2010).

[52] Robinson, J., Uysal, M., Swaminathan, R., and Knightly, E. Adding capacity points to a wireless mesh network using local search. In *IEEE INFOCOM* (2008).

[53] Rosston, G., Savage, S., and Waldman, D. Household demand for broadband internet service. *Communications of the ACM 54*, 2 (2011), 29–31.

[54] Sabharwal, A., Khoshnevis, A., and Knightly, E. Opportunistic spectral usage: Bounds and a multi-band csma/ca protocol. *Networking, IEEE/ACM Transactions on 15*, 3 (2007), 533–545.

[55] Sadeghi, B., Kanodia, V., Sabharwal, A., and Knightly, E. Opportunistic media access for multirate ad hoc networks. In *ACM MobiCom* (Sept. 2002).

[56] Shellhammer, S., Sadek, A., and Zhang, W. Technical challenges for cognitive radio in the tv white space spectrum. In *Information Theory and Applications Workshop, 2009* (2009), IEEE, pp. 323–333.

[57] Si, W., Selvakennedy, S., and Zomaya, A. Y. An overview of channel assignment methods for multi-radio multi-channel wireless mesh networks. *Journal of Parallel and Distributed Computing 70*, 5 (2010), 505–524.

[58] Subramanian, A. P., Gupta, H., Das, S. R., and Cao, J. Minimum interference channel assignment in multiradio wireless mesh networks. *IEEE TMC 7*, 12 (2008), 1459–1473.

[59] Tang, J., Xue, G., and Zhang, W. Interference-aware topology control and QoS routing in multi-channel wireless mesh networks. In *ACM MobiHoc* (2005).

[60] Wang, B., Wu, Y., and Liu, K. Game theory for cognitive radio networks: An overview. *Computer Networks 54*, 14 (2010), 2537–2561.

[61] Wu, H., Yang, F., Tan, K., Chen, J., Zhang, Q., and Zhang, Z. Distributed channel assignment and routing in multiradio multichannel multihop wireless networks. *Selected Areas in Communications, IEEE Journal on 24*, 11 (2006), 1972–1983.

[62] Wu, X., Liu, J., and Chen, G. Analysis of bottleneck delay and throughput in wireless mesh networks. In *IEEE MASS* (2006).

[63] Yuan, J., Li, Z., Yu, W., and Li, B. A cross-layer optimization framework for multihop multicast in wireless mesh networks. *IEEE JSAC 24*, 11 (2006), 2092–2103.

[64] Zhang, H., Berg, A., Maire, M., and Malik, J. Svm-knn: Discriminative nearest neighbor classification for visual category recognition. In *Computer Vision and Pattern Recognition, 2006 IEEE Computer Society Conference on* (2006), vol. 2, pp. 2126–2136.